

## Article (refereed) - postprint

---

Bell, V.A.; Kay, A.L.; Cole, S.J.; Jones, R.G.; Moore, R.J.; Reynard, N.S. 2012  
How might climate change affect river flows across the Thames Basin?: an  
area-wide analysis using the UKCP09 Regional Climate Model ensemble.  
*Journal of Hydrology*, 442-443. 89-104. [10.1016/j.jhydrol.2012.04.001](https://doi.org/10.1016/j.jhydrol.2012.04.001)

Crown Copyright © 2012 Published by Elsevier B.V.

This version available <http://nora.nerc.ac.uk/17851/>

NERC has developed NORA to enable users to access research outputs wholly or partially funded by NERC. Copyright and other rights for material on this site are retained by the rights owners. Users should read the terms and conditions of use of this material at <http://nora.nerc.ac.uk/policies.html#access>

NOTICE: this is the author's version of a work that was accepted for publication in *Journal of Hydrology*. Changes resulting from the publishing process, such as peer review, editing, corrections, structural formatting, and other quality control mechanisms may not be reflected in this document. Changes may have been made to this work since it was submitted for publication. A definitive version was subsequently published in *Journal of Hydrology*, 442-443. 89-104. [10.1016/j.jhydrol.2012.04.001](https://doi.org/10.1016/j.jhydrol.2012.04.001)

[www.elsevier.com/](http://www.elsevier.com/)

Contact CEH NORA team at  
[noraceh@ceh.ac.uk](mailto:noraceh@ceh.ac.uk)

# 1 **How might climate change affect river flows across the** 2 **Thames Basin? An area-wide analysis using the UKCP09** 3 **Regional Climate Model ensemble**

4  
5 V.A. Bell<sup>1</sup>, A.L. Kay<sup>1</sup>, S.J. Cole<sup>1</sup>, R.G. Jones<sup>2</sup>, R.J. Moore<sup>1</sup> and N.S.Reynard<sup>1</sup>

6  
7 <sup>1</sup>Centre for Ecology and Hydrology, Wallingford, Oxfordshire, OX10 8BB, UK

8 <sup>2</sup>Met Office Hadley Centre (Reading Unit), Meteorology Building, University of Reading,  
9 Reading, RG6 6BB, UK

10  
11 Corresponding author: Tel: +44 1491 692264; Fax: +44 1491 692424

12 E-mail address: [vib@ceh.ac.uk](mailto:vib@ceh.ac.uk) (V.A. Bell).

## 13 14 **Abstract**

15 The Thames Basin drains an area of over 10,000km<sup>2</sup> through London to the North Sea. It  
16 encompasses both rural and heavily urbanised areas overlying a spatially-varied and complex  
17 geology. Historically, the lower Thames has proved resilient to climate variability, and careful  
18 river management in recent years has helped protect the region from flooding. However,  
19 recent climate projections for the region indicate that over the next century winter rainfall  
20 might increase by 10-15%, potentially leading to higher flows than the Thames can  
21 accommodate. This study uses a distributed hydrological model, the Grid-to-Grid (G2G), to  
22 assess future changes in peak river flows for a range of catchments across the Thames Basin.  
23 The G2G model has used as input an ensemble from the UK Climate Projections (UKCP09)  
24 Regional Climate Model (RCM), under the A1B emissions scenario, to analyse changes in  
25 flood frequency between two 30-year time-slices (Oct 1960-Sep 1990 and Oct 2069-Sep  
26 2099). The RCM ensemble uses a perturbed-parameter approach to address uncertainty in  
27 climate projections.

28  
29 Results indicate considerable spatial variation in projected changes in peak flows. Towards  
30 the downstream end of the fluvial Thames, the average estimated change in modelled 20-year  
31 return period flood peaks by the 2080s is 36% with a range of -11% to +68%, which is  
32 broadly in line with recent government guidance for the Thames Basin. A key question that  
33 arises is whether these estimated changes fall within the range of natural variability and would  
34 therefore be indistinguishable from the effects of typical weather patterns in the current  
35 climate. Comparison of the modelled changes in flood frequency with an RCM-based  
36 estimate of current natural variability shows that, whilst for some rivers (or parts of rivers)  
37 there are few changes outside the range of current natural variability, for other rivers there are  
38 more changes outside of this range. The latter locations could be considered as sites where  
39 further monitoring/modelling may provide early warning of statistically significant changes in  
40 observed flows, due to climate change.

# 1 **Keywords**

2 Rainfall-runoff, flood frequency, climate change, RCM ensemble, UK Climate Projections  
3 2009

## 4 **1 Introduction**

5 Since the 1960s, daily precipitation in the UK has tended to be more intense in winter and less  
6 intense in summer (Osborn and Hulme, 2002; Maraun et al., 2008). The impact of changes in  
7 rainfall on river flows will depend on both the nature of the rainfall and the physical  
8 characteristics of the catchment draining to the river. For fast-responding catchments, such as  
9 those in impermeable or high relief areas, the characteristics of the specific rainfall event are  
10 critical. These fast-responding catchments tend not to have the deep soils or permeable  
11 geology that lead to the long-term hydrological “memory” of larger lowland catchments.  
12 Catchments across the Thames Basin in England are typical of these lowland catchments,  
13 where the longer-term balance between rainfall and evaporation is particularly important. The  
14 River Thames is of particular strategic importance as it drains an area of over 10,000 km<sup>2</sup>  
15 through central London, much of which was developed on low-lying marshland close to the  
16 Thames Estuary (Fig. 1). The Thames Barrier provides flood protection from tidal surges  
17 which are the main threat, but extremes of fluvial flow will also have an impact on thousands  
18 of properties situated in the flood plain.

Fig. 1

19  
20 Historically, the lower Thames has proved resilient to climate variability. There is no long-  
21 term trend in annual maximum flows over the 126 year record for the Thames (Marsh 2004),  
22 despite increases in temperature and a major change in the seasonal partitioning of rainfall.  
23 River management in recent times (for example channel straightening, bed re-profiling, and  
24 improvements to the efficiency of weirs) has led to greater channel storage and conveyance.  
25 This has resulted in fewer floods in the lower Thames. At Kingston, for example, an increase  
26 of around 30% in the channel capacity over the last 70 years means that flows that would  
27 have caused significant flooding in the 1930s can now be accommodated within-bank.

28  
29 In the recent IPCC assessment (IPCC 2007) of projected climate change over Europe a wide  
30 range of changes in precipitation is seen over the UK. By the 2080s under the A1B (medium)  
31 emissions scenario, this includes winter rainfall increases of up to 15% and summer rainfall  
32 decreases of up to 20% over England. The UK Climate Projections (UKCP09) incorporate  
33 information assessed by the IPCC along with projections from a larger ensemble of Hadley  
34 Centre global and regional models and estimate, for the same emissions scenario and future  
35 time period, a 50% probability of winter rainfall increasing by 19% and summer rainfall

1 decreasing by 22% for the London area (Jenkins et al., 2009). It should also be noted that both  
2 sets of projections include much smaller increases in winter precipitation and increases in  
3 summer precipitation. Coupled with projected increases in mean temperature of 3-4K which  
4 could affect evaporation, the overall impact of these changes on river flows is unclear.

5  
6 Most research into the effects of climate change on UK river flows has used catchment  
7 hydrological models to provide estimates of changes in flow at single locations or a small set  
8 of locations (e.g. Kay et al., 2009; New et al., 2007; Fowler and Kilsby, 2007; Wilby and  
9 Harris, 2006; Wilby et al., 2006; Nawaz and Adeloje, 2006; Cameron, 2006; Kay et al., 2006;  
10 Arnell, 2003; Reynard et al., 2001). Normally, the hydrological model is calibrated to  
11 catchment conditions, using model parameters to adjust the modelled catchment response to  
12 rainfall, in order to reproduce the controlling effects of spatial heterogeneity of  
13 soil/geology/topography. The model parameters can also be adjusted to take into account  
14 artificial influences on flows, such as abstraction. Using this approach, Kay et al. (2006)  
15 examined the effect of projected climate change on river flows for 15 catchments across the  
16 UK using a simplified form of the PDM catchment model whose parameters were estimated  
17 using derived regression relationships with catchment properties provided by digital datasets  
18 (e.g. land cover, soil-type). An RCM assuming a UKCIP02 climate scenario (Hulme et al.,  
19 2002) provided the atmospheric inputs to the PDM and, despite decreases in average annual  
20 rainfall in most catchments, eight catchments showed an increase in flood frequency at most  
21 return periods while two showed substantial decreases (one of which was located in the  
22 Thames Basin). The increases in flood frequency, despite decreased annual rainfall, were  
23 attributed to the UKCIP02 projection of increased seasonality in future rainfall with more  
24 rainfall falling in winter.

25  
26 Distributed grid-based models provide another approach to understanding the spatial effects  
27 of projected climate change on river flows, and can potentially provide flow estimates for all  
28 locations on a spatial grid including ungauged sites. An important strength is their use of  
29 digital datasets of terrain/soil/geology/land-cover properties to underpin the model response to  
30 rainfall and potential evaporation (PE). Land-surface models are of this type; their  
31 development was motivated by Global Climate Models (GCMs) which required estimates of  
32 fluxes of heat and water vapour between the land-surface and atmosphere. These models can  
33 provide estimates of soil-moisture, runoff and river flow, but often on a coarse grid and at a  
34 monthly time-step (although the resolution is increasing), with global coverage. In recent  
35 years, the hydrological modelling community has in turn moved to larger scales with the  
36 development of gridded hydrological models which rely on now widely-available spatial  
37 datasets on landscape properties to control spatial heterogeneity of catchment response. Often

1 using as inputs climate model outputs, these hydrological models provide a means to estimate  
2 the impact of regional climate change on river flow response at a regional or large-catchment  
3 scale. National-scale hydrological models are now emerging: for example Henriksen et al.,  
4 (2003) present and assess a hydrological model for Denmark based on the MIKE SHE model  
5 (Abbott et al., 1986). Another grid-based model, LISFLOOD, has been developed and applied  
6 to simulate river flow, soil-moisture and flood inundation in large European river basins (De  
7 Roo et al., 2000, 2003).

8  
9 The work presented here uses a single model (Grid-to-Grid, or G2G) and set of parameters for  
10 the whole of the Thames Basin (~13600 km<sup>2</sup>), employing digital datasets to provide the  
11 spatial information needed to simulate spatial differences in the flow response to rainfall  
12 across the river basin. G2G output consists of a (1km) grid of river flow estimates across the  
13 region of application. The G2G can either be used as an area-wide model providing flow  
14 estimates over a large region, or as a catchment model which may be calibrated to obtain the  
15 best possible agreement between modelled and observed flows. As an area-wide model, the  
16 G2G can be less accurate for a particular catchment than a model specifically calibrated to the  
17 catchment, but is well suited to support river flow simulation at any set of locations within a  
18 region. Bell et al., (2009) assessed the G2G model performance for 43 catchments across  
19 Britain using daily rainfall and river flow observations, finding that it provided reasonably  
20 good daily flow estimates. For the smaller Thames Basin area examined here, model  
21 parameters which govern the temporal development of flow peaks have been determined  
22 through recalibration using 15-minute time-series of rainfalls and river flows, while taking  
23 care not to over-calibrate the model to individual catchments. Model performance has been  
24 assessed with reference to quality-controlled river flow records for 34 locations across the  
25 area.

26  
27 To estimate projected future changes in peak river flows, the calibrated Thames G2G model  
28 employs as its input rainfall and PE estimates derived from outputs from a 25 km resolution  
29 RCM, for a Current (Oct 1960 to Sep 1990) and a Future (Oct 2069 to Sep 2099) time-slice.  
30 The RCM used here consists of the Met Office Hadley Centre perturbed-physics ensemble of  
31 11 variants of the RCM (HadRM3), run from 1950-2099 and used to dynamically downscale  
32 GCM results as part of the latest UK Climate Projections report (Jenkins et al., 2009). The  
33 broader aim of this study was to produce estimates of spatial changes in return period flows  
34 on a continuous 1 km grid across the Thames Basin, to support future flood defence planning.  
35 Estimating changes to the inflows to the tidal Thames via the main river and 13 major  
36 tributaries is of particular interest to future planning in relation to the Thames Barrier.

37

1 A key question that arises is whether these estimated flow changes fall within the range of  
2 natural variability and would therefore be indistinguishable from changes arising from typical  
3 weather pattern variation. Here an RCM ensemble representative of “present climate” has  
4 been used to provide an estimate of natural variability with which modelled changes in flood  
5 frequency can be compared. Areas within the Thames Basin where projected climate change  
6 impacts on river flows fall outside this estimated range of natural variability will be  
7 investigated and highlighted.

## 8 **2 Hydrological Modelling**

### 9 **2.1 The Grid-to-Grid model**

10 The hydrological model used here is a distributed model of runoff production and flow  
11 routing - called the Grid-to-Grid (or G2G) - formulated to employ terrain, soil/geology and  
12 land-cover datasets, presented as the “Soil-G2G” in Bell et al., (2009). The model formulation  
13 contains enhancements to the prototype G2G formulation previously trialled in the Upper  
14 Thames catchments (Moore et al., 2006, 2007), which was in turn a development of the  
15 elevation-dependent formulation presented in Bell et al., (2007a,b) and extended by Cole and  
16 Moore (2009). The model formulation is presented briefly here and further detail is provided  
17 by Bell et al., (2008, 2009), together with an assessment for a large range of UK catchments.

18

19 The G2G model is modular in form and distinguishes between runoff-production and lateral  
20 routing of runoff to form river flow. The runoff-production scheme divides the terrain into a  
21 square grid of vertical soil columns which are subject to precipitation and evaporation. Some  
22 of the rainwater entering the soil column can drain laterally to adjacent grid-squares, while  
23 saturation-excess flow contributes to surface runoff. Water also moves downwards via  
24 percolation and drainage which eventually contributes to groundwater (sub-surface) flow. In  
25 order to ensure that a grid-square generates realistic quantities of saturation-excess surface  
26 runoff even when it is not fully saturated, a probability-distributed soil moisture store  
27 formulation (Moore, 1985, 2007; Zhao et al., 1980) has been invoked within each grid-square.  
28 This conceptualisation represents the spatial variation in water absorption capacity with soil,  
29 geology, land-cover and topography across the grid-square.

30

31 Digital datasets are used to provide estimates of soil hydraulic properties required by the  
32 runoff-production scheme. These soil properties are specified where possible through a  
33 relationship between the HOST (Hydrology of Soil Types) classification of soils (Boorman et  
34 al., 1995) and highly derived soil attributes. For each of the 29 HOST soil classes (of which  
35 only nine classes have a significant presence in the Thames Basin), an association table

1 provides indicative estimates of the saturation and residual water contents, the vertical  
2 saturated hydraulic conductivity, and the depth of the soil column. These soil property  
3 estimates offer only a coarse approximation for use at the model scale (1km and depth  
4 integrated) and cannot reflect the true spatial complexity of soil water control. However, the  
5 modest number of soil classes involved has the advantage of easing exploration of how soil  
6 properties impact on the timing and volume of runoff-production across the Thames Basin.

7

8 Digital datasets are also used to configure and parameterise lateral routing of runoff across the  
9 landscape to form estimates of river flow. Flow-routing is undertaken in two parallel planes  
10 representing sub-surface and surface pathways with a return flow term representing the  
11 contribution of groundwater to river flow. The gridded flow-directions which define the  
12 lateral pathways of water movement constitute a critical component of the model  
13 configuration as they determine the water-balance contributing to flow at every location. The  
14 network-derivation scheme of Paz et al. (2006) has been used to identify 1km-resolution flow  
15 directions from hydrologically-corrected 50m river networks, following the recommendations  
16 of Davies and Bell (2008) who found that use of this scheme resulted in the smallest errors in  
17 derived catchment area when compared to other methods. For the set of Thames catchments  
18 examined here, errors in derived area are usually less than 5%, and less than 1% for more than  
19 half the catchments.

20

21 Schemes that invoke the kinematic wave approximation in their development form the basis  
22 of the routing component of G2G. Routing along surface land pathways and subsurface land  
23 and river pathways employs kinematic wave equations, applied in 1-dimension over a 2-  
24 dimensional river network and approximated by a finite-difference scheme (Bell et al.,  
25 2007a,b). The wave speed can vary with the pathway (surface or subsurface) and surface-type  
26 (land or river) combination. Routing along surface river pathways employs the Horton-Izzard  
27 nonlinear storage approach (Dooge, 1973; Moore and Bell, 2001) applied to a varying width  
28 channel network (Ciarapica and Todini, 2002; Moore et al., 2007) and exploits  
29 geomorphological relations developed by Bell and Moore (2004). In urban and sub-urban  
30 areas - identified through the LCM2000 spatial dataset of land-cover (Fuller et al., 2002) -  
31 responsiveness has been increased through the use of an enhanced routing speed and reduced  
32 soil storage, leading to a faster response to rainfall.

33

34 **2.2 The Thames Basin**

35 Both soil and geology influence the hydrological response of catchments to rainfall. The  
36 geology of the Thames Basin is particularly complex with many catchments comprising a

1 mixture of geological types, as shown in Fig. 2(a). A main feature of the region is the chalk  
2 escarpment of the Chilterns running southwest to northeast, also evident in the relief map of  
3 Fig. 2(b). The escarpment is broken in places by valleys, in particular by the Thames at  
4 Goring Gap (situated south of gauging station 39139). The remainder of the Thames Basin is  
5 made up of newer rocks with superficial deposits. London is situated to the eastern side of the  
6 basin, in a depression in the underlying chalk over which sand and London Clay have been  
7 deposited. The north-western catchments are underlain by Liassic formations, with a majority  
8 being clay, in particular Lias Clay to the north of Banbury (39026). A band of Great Oolite, a  
9 sedimentary rock, sometimes called clayey limestone, underlies catchments such as the  
10 Windrush (39006), the Evenlode (39034) and the Northern part of the Thames to Farmoor  
11 (39129). The underlying geology influences both the relief and the soils in the catchment  
12 above: areas of higher relief tend to correspond to chalk and marlstone geology. Soil consists  
13 of a mixture of weathered rock and organic matter, both of which influence its properties.

14

15 The relationship between catchment response and geology is highlighted in Table 1 which  
16 lists the 34 study catchments in decreasing order of baseflow index (BFI) which is closely  
17 associated with soil and geology, with deeper soils (or permeable bedrock) resulting in a  
18 larger baseflow response (Gustard et al., 1992). The table indicates that in this region,  
19 catchments with low BFI ( $<0.4$ ) tend to overlay London Clay. These catchments tend to have  
20 shallower soils above an impermeable or “gleyed layer” and respond relatively quickly to  
21 rainfall events. High BFI ( $>0.7$ ) is associated with chalk/Lias geological formations which  
22 tend to have deeper soil-stores or aquifers and a slower response to rainfall. The Lias group of  
23 rocks generate a surprisingly large range of overlying soil properties with effective soil depths  
24 ranging from 0.31m in the Ray at Grendon (39017) to 0.54m in the Cherwell at Enslow Mill  
25 (39021). This variation can be attributed to the further classification of Lias group rocks into  
26 Lower and Middle Lias formations which have very different properties: the Middle Lias  
27 group consists of deep silts and fine sandstones overlain by the relatively thin sandstone and  
28 ironstone of the Marlstone Rock Formation, while the Lower Lias group, consists  
29 predominantly of mudstones over an impervious layer of limestone.

30

31 The spatially-distributed nature of the G2G model allows for river flow simulation to be  
32 undertaken for an entire region or for individual catchments for which observations of river  
33 flows are available for calibration and assessment. Here, the G2G has been applied at a  
34 regional scale in order to give consistent, area-wide estimates of the effects of projected  
35 climate change on river flows across the Thames Basin. Many centuries of development in the  
36 Thames Basin makes it difficult to find catchments entirely free from anthropogenic changes  
37 to the flow regime: thus a high proportion of artificially-influenced catchments are included

1 here in the model assessment. These influences are taken into consideration during model  
2 calibration and assessment, noting that the G2G formulation used here will perform best in  
3 natural river basins.

4  
5 In their study of high-flow trends in undisturbed UK catchments, Hannaford and Marsh  
6 (2008) note that “very few UK rivers are pristine”, but are able to identify a number of  
7 catchments for which the net influence of artificial disturbance is modest. This list is subject  
8 to ongoing revision and Table 1 highlights that six of the 34 study catchments are at present  
9 considered to be relatively undisturbed. Thus for these catchments a more accurate simulation  
10 of observed flows may be achievable with the simple model formulation used here. The flow  
11 regimes of the other 28 catchments are more heavily influenced, with factors ranging from a  
12 reduction in flow from groundwater abstraction (39026, 39129, 39046, 39005, 39010, 39056,  
13 39001, 40016, 40012), to increases in measured flows from effluent returns (39034, 39021,  
14 39046, 39010, 39069, 39005, 39007, 39003) or augmented low-flows (39049, 40012).  
15 However, many catchments are affected by abstraction to a lesser degree, whilst the variable  
16 accuracy of gauged river flows beyond bankfull capacity affects estimation of high flow  
17 peaks in others. Further model development to include (at least) abstractions could  
18 significantly improve simulation accuracy in the Thames Basin.

### 20 **2.3 Model calibration and assessment**

21 Previous work has examined the performance of the G2G for catchments across the UK using  
22 daily rainfall and river flow records (Bell et al., 2009). For a country-wide analysis, daily  
23 records are more readily available than those at 15 minute resolution, but for the Thames  
24 Basin it has been possible to assemble concurrent flow and rainfall data at the finer resolution.  
25 These data derive from 15 minute rainfall accumulations, obtained from a dense network of  
26 103 tipping-bucket raingauges, and interpolated onto a 1km grid using a multi-quadric surface  
27 fitting technique (Cole and Moore, 2008, 2009). Gridded estimates of potential evaporation  
28 from a short grass vegetated surface are provided by MORECS (Met Office Rainfall and  
29 Evaporation Calculation System), a monthly climatological dataset for 201 (40 by 40 km)  
30 squares across the UK (Thompson et al., 1982; Hough et al., 1997). The combined potential  
31 evaporation from land and vegetation is sometimes referred to as “potential  
32 evapotranspiration” (PET), but here the abbreviation PE will be used in preference. Model  
33 performance has been assessed with reference to quality-controlled river levels/flows  
34 provided by the Environment Agency for 34 locations in the Thames Basin at a 15 minute  
35 resolution. A complete list of the gauging stations and the area draining to them is presented  
36 in Table 1.

1

2 Five years of records (January 1997 to December 2001) were used for split sample calibration  
3 and assessment, although periods of missing data have reduced the record-length in places.  
4 For calibration, the G2G model was initialised from 1 January to 21 July 1999 and then run  
5 from 21 July 1999 to 18 June 2001; for assessment, the model was initialised from 1 January  
6 to 21 July 1997 and then run from 21 July 1997 to 18 June 1999. To maximise use of good  
7 quality records there is an overlap in the two datasets during initialisation of the calibration  
8 period. Model performance over this initialisation period is ignored by the calibration process  
9 so these data are considered to be available for the independent model assessment.

10

11 The G2G was designed to rely on digital datasets to determine the response of the landscape  
12 to rainfall. However, many aspects of sub-surface hydrology are ill-defined, leading to the  
13 need to adjust or “calibrate” some model parameters to gain better agreement between  
14 observed and modelled river flows. Here, the seven routing parameters which govern the  
15 temporal development of flow peaks are set at a regional level (in this case the whole of the  
16 Thames Basin) while the heterogeneity of runoff production is specified primarily through the  
17 spatial datasets of slope, urban land-cover and soil properties, leaving only two regional  
18 parameters relating to runoff requiring adjustment. These two runoff parameters provide  
19 regional estimates of the vertical saturated hydraulic conductivity and the groundwater  
20 drainage rate constant, while the routing parameters comprise four lateral routing parameters  
21 (for surface and sub-surface, land and river routing), land and river return flow factors, and a  
22 critical drainage area beyond which flow in a 1km grid-cell is assumed to be river. In practice,  
23 accurate flow simulation is most dependent on the two runoff parameters: the return flow term  
24 and the surface river flow routing parameter. Values for all the parameters are determined by  
25 manual calibration to river flow records for locations across the Thames Basin. Future  
26 developments using improved spatial datasets will aim to strengthen the underpinning  
27 physical basis of the model, reducing reliance upon model calibration.

28

29 The G2G model is designed for area-wide use, so care has been taken not to over-calibrate the  
30 model to individual catchments. Instead, river flow records for catchments with a  
31 predominant soil-type have been used to determine whether the soil hydraulic properties  
32 associated with the HOST soil-type provide realistic estimates of the relative volumes of  
33 surface- and sub-surface runoff. Where required, manual adjustment of soil hydraulic  
34 properties (usually effective soil depths) is applied recursively to different catchments and  
35 sub-catchments until a good estimate of downstream surface- and base-flow volumes across a  
36 range of soil-types is achieved. In the Thames Basin nine HOST soil types have a significant  
37 presence, of which four classes - 1 and 18 (soils overlying chalk), 25 (clay) and 2

1 (limestone/marlstone) - are most dominant. It is these soil types for which some adjustment  
2 has been made with respect to the effective soil depth. In chalk areas, the baseflow component  
3 of river flow depends on the volume of water stored in both the soil and the aquifer. On  
4 account of the lack of data on groundwater hydraulic properties, storage in these areas has  
5 been augmented by increasing the effective soil depth to a value larger than is typically  
6 observed and assuming that the soil hydraulic properties apply at all depths. This procedure  
7 results in depths of 3.0m and 2.0m for HOST classes 1 and 18 respectively (previously 0.73m  
8 and 0.91m respectively). Similarly, the soil depth (to a gleyed layer) in clay soils has been  
9 decreased from 0.25m to 0.15m to speed up the hydrological response in clay soils; however,  
10 since much urban development has taken place on London Clay it has been hard to separate  
11 the two factors.

12  
13 Calibration and assessment results for 34 catchments are presented in Fig. 3, displayed in  
14 descending order of BFI for both undisturbed and anthropogenically-influenced catchments.  
15 Model performance is evaluated for 15-minute flows and summarised in terms of  $R^2$   
16 Efficiency, as defined by Nash and Sutcliffe (1970); this provides a relative measure of model  
17 simulation accuracy permitting some comparison across the different catchments. A value of  
18 1 indicates perfect agreement, 0 indicates the model simulation is only as good as using the  
19 mean flow value for the whole period, whilst negative values arise if the flow simulations are  
20 worse than that provided by the mean flow. Negative  $R^2$  values are indicated with a value of -  
21 0.1 in Fig. 3 for clarity of display, but can be as poor as -8.0 for catchments subject to  
22 anthropogenic influences (e.g. the Darent, which is subject to groundwater abstraction,  
23 augmented low flows and an erroneous sub-surface contributing area).

Fig. 3

24  
25 The G2G model has the best performance statistics when applied to catchments for which (a)  
26 the response to rainfall is relatively free from artificial influences, (b) the gauge is considered  
27 to be reasonably accurate and (c) there are no significant data problems (flow and rainfall). In  
28 these areas,  $R^2$  Efficiency ranges from 0.59 to 0.84 (median 0.77) for the calibration period  
29 and from 0.40 to 0.77 (median 0.75) for the assessment period. For catchments with greater  
30 levels of anthropogenic disturbance, G2G model simulation accuracy is more variable,  
31 usually in line with the degree of disturbance. For these catchments,  $R^2$  Efficiency ranges  
32 from -2.89 to 0.85 (median 0.55) for the calibration period, and from -8.0 to 0.84 (median  
33 0.33) for the assessment period. Example hydrographs for four catchments over the two-year  
34 assessment period are presented in Fig. 4. Hydrograph (a) for the Ock at Abingdon (39081)  
35 provides an example of a catchment where the G2G is performing reasonably well, although  
36 some peaks are overestimated. The hydrograph for the Lambourn at Shaw (39019) shows how  
37 the G2G performs for a groundwater-dominated chalk catchment with only limited net

Fig. 4

1 artificial disturbance to the natural flow regime. Here, observed and modelled flows are not  
2 co-incident but they are similar, and the configuration of the G2G model has enabled its  
3 response in this catchment to be very different to (say) the Ock at Abingdon. The G2G model  
4 simulates natural rather than influenced flows and thus can appear to over- or under-estimate  
5 flows for heavily influenced catchments (e.g. those affected by effluent returns or abstractions  
6 for public water supply). Hydrograph (c) for the Darent at Hawley (40012) provides an  
7 example of where the G2G struggles to simulate observed flows because of anthropogenic  
8 influences discussed earlier. Hydrograph (d) presents simulated and observed flows for the  
9 Thames to Kingston (39001) alongside naturalised flows which are adjusted to take account  
10 of net abstractions and discharges upstream of the gauging station. The flows are shown as  
11 daily mean values (naturalised flows are not available at a 15-minute resolution) and the  
12 graph indicates that naturalised flows are generally higher for this catchment than observed  
13 flows particularly during the summer months. As expected, flows simulated by the G2G are  
14 much closer to naturalised flows than observed. For the Thames to Kingston, daily  $R^2$   
15 Efficiency values increase from 0.78 to 0.84 for the calibration period and from 0.20 to 0.51  
16 for the assessment period when modelled flows are compared to naturalised rather than  
17 observed flows. Overall, these hydrographs indicate that the G2G model is able to broadly  
18 reproduce a wide range of hydrological behaviour in catchments which have very different  
19 responses to rainfall.

20

21 Against the background of this assessment of G2G model performance for historical periods,  
22 the model is used here with some confidence to investigate the impact of projected climate  
23 change on flood frequency for naturalised flows across the Thames Basin. Although for a  
24 particular catchment the G2G does not perform as well as a model specifically calibrated to  
25 flows gauged at its outlet, the G2G has been shown to be able to reflect the heterogeneity of  
26 response to rainfall from different landscapes in a consistent way across the whole region.  
27 Climate change impacts on river flows for a particular catchment should however be  
28 considered indicative only: they do not reflect current (or future) flood defences, flood  
29 inundation or anthropogenic influences. Importantly, this analysis can serve to highlight areas  
30 that may be particularly sensitive to projected changes in the rainfall regime and that deserve  
31 further investigation in support of flood defence planning.

## 32 **3 Use of Regional Climate Model (RCM) data**

### 33 **3.1 The Hadley Centre RCM**

34 Gridded rainfall and potential evaporation estimates from a system consisting of the Met  
35 Office Hadley Centre GCM, HadCM3, dynamically downscaled to 25km using the HadRM3

1 RCM are used to as input to the G2G hydrological model. HadCM3 (Gordon et al., 2000;  
2 Pope et al., 2000) has previously been shown to have considerable skill at simulating the  
3 global climate. Furthermore, when combined with the regional atmospheric climate model  
4 HadRM3, a higher resolution version of the atmospheric component of HadCM3, the  
5 modelling system is able to reproduce many of the observed features of the United Kingdom  
6 and European climate (see e.g. Jones et al., 2004; Buonomo et al., 2007).

7  
8 The HadRM3 perturbed physics experiment (HadRM3-PPE-UK) was designed to simulate the  
9 regional climate for the UK in the period 1950-2100 using historical emissions and a medium  
10 (SRES A1B) emissions scenario, and is a key UK Climate Projections dataset (UKCP09;  
11 Murphy et al., 2009). This RCM ensemble is the dynamical downscaling component of an 11-  
12 member ensemble of global and regional models where the global model provides boundary  
13 conditions to the RCM whose formulation matches that of its driving GCM. One member of  
14 the ensemble comprises the GCM/RCM pair HadCM3/HadRM3 and the other 10 members  
15 are formed of GCM/RCM pairs incorporating a range of perturbations to important  
16 parameters in the physical formulation of the HadCM3/HadRM3 models. The same historical  
17 (1950-2000) and future (2000-2100) climate forcings from the SRES A1B scenario (IPCC,  
18 2000) were used in each of the GCM/RCM pairs. The standard forcings include historical  
19 levels of greenhouse gases (including methane), sulphur (direct and first indirect forcing,  
20 sulphur chemistry without natural DMS and SO<sub>2</sub> background emissions; anthropogenic SO<sub>2</sub>  
21 emissions from surface and high level only) and tropospheric/stratospheric ozone.

22  
23 RCM output data are available on a 0.22° (~25km) rotated lat-long grid, shown in Fig. 1. The  
24 data comprise hourly precipitation and daily PE data, which are then downscaled to a 1 km  
25 UK national grid as required by the G2G model. Since rainfall is highly spatially variable, the  
26 Standard Average Annual Rainfall (SAAR) 1km dataset for the UK for the period 1961-1990  
27 has been used for downscaling using the approach outlined in Bell et al. (2007a). For each  
28 time-step, the rainfall for each RCM grid-square is multiplied by the ratio of RCM grid-  
29 square SAAR to the 1 km grid-square SAAR to provide rainfall on a 1 km grid. This  
30 determines whether some areas generally receive more or less rainfall than others, for instance  
31 as a consequence of topography, but makes no attempt to adjust overall rainfall amounts in  
32 line with observations. The same SAAR weighting is used for both the Current and Future  
33 time-slices of the RCM precipitation data (with an assumption that there will be no major  
34 changes in the track of weather systems). Note that although the RCM precipitation is  
35 available at an hourly time-step, it is applied within the G2G at a 15-minute time-step by  
36 dividing each hourly value by four.

37

1 The G2G requires as input an estimate of PE for a short grass land-cover. Currently, where an  
2 estimate of PE from vegetation is required for use in impact studies, it is common  
3 hydrological practice to use climate model outputs of atmospheric variables as input to a  
4 standard PE estimation scheme. These schemes vary in complexity and data requirements,  
5 ranging from temperature-only methods such as those used by Thornthwaite (1948) and  
6 Oudin et al. (2005) to the full Penman-Monteith formulation (Monteith, 1965) requiring  
7 estimates of air temperature, relative humidity, wind-speed and net downward short- and  
8 long-wave radiation. The more complex schemes are often preferred for climate impact  
9 studies as their physical basis is likely to be more responsive to climate effects on a range of  
10 atmospheric variables. One of the climate model parameter perturbations of particular  
11 relevance to hydrological applications is the dependence of stomatal conductance on  
12 atmospheric CO<sub>2</sub> levels. This effect has been included in six of the 11 ensemble members and  
13 may be an important consideration for climate impact and modelling studies as increased CO<sub>2</sub>  
14 is thought to lead to leaf stomatal closure and a reduction in evaporation from vegetated  
15 surfaces. Recent studies, such as Gedney et al. (2006), indicate that elevated levels of  
16 atmospheric CO<sub>2</sub> can reduce evaporation from vegetation which could result in river flow  
17 increasing under projected climate change. The method of Bell et al. (2011) has been used  
18 here to estimate PE from vegetated surfaces using a scheme which emulates that of Penman-  
19 Monteith and can take advantage of RCM estimates of the effect of projected future change in  
20 CO<sub>2</sub> levels on plant stomata. Note that although the PE estimates derived from the RCM data  
21 are available at a daily time-step, they are used within the G2G at a 15-minute time-step by  
22 spreading each daily total equally throughout the day.

23

24 For each ensemble member, data for two time-slices were chosen out of the full 150-year  
25 RCM run. The first (Current) time-slice runs from 1 October 1960 to 30 September 1990 and  
26 the second (Future) time-slice runs from 1 October 2069 to 30 September 2099. Note that  
27 both time-slices have been chosen so as to cover exactly 30 water-years, although it should be  
28 noted that the length of an RCM year is only 360 days, comprising of twelve 30-day months  
29 (which is applied in the climate modelling system to simplify the run-time calculation of  
30 monthly and seasonal statistics). The G2G model was run for each time-slice *including* a 9-  
31 month run-in period before each (i.e. from 1 January 1960 and 1 January 2069 for Current and  
32 Future respectively).

33

## 3.2 Comparison between RCM estimates and observations

### 3.2.1 Rainfall and PE

It is useful to compare the ensemble RCM precipitation and PE both between the Current and Future time-slices for each ensemble member, to assess how the G2G model inputs are changing between the two time-slices, and with observational series, to aid an assessment of the performance of each member individually and of the ensemble as a whole. However, it should be noted that any comparison of RCM data with observational data needs to be interpreted with care, as the Current run of each ensemble member is not meant to reproduce exactly what happened in that period, but is simply one possible representation of what *could* have happened in that period, given the existence of stochasticity and natural variability. In addition, differences in resolution between RCM grids and observational grids could cause discrepancies, particularly for rainfall and especially in regions with high topographic variability.

Fig. 5 shows, for one RCM grid-box located in the north of the Thames Basin (indicated by the highlighted box in Fig. 1), the monthly mean rainfall and PE over each time-slice, and the difference between the two time-slices, for each ensemble-member. The unperturbed ensemble member is shown with a bold black line and the dashed black line indicates observed rainfall and PE for the period 1961 to 1990. The observed rainfall has been taken from a corresponding box within the dataset of Met Office 5km grid-interpolated daily rainfall. The ‘observed’ PE has been taken from a corresponding location within the MORECS dataset of 40km gridded monthly mean PE. The graphs highlight the variability between the 11 ensemble members but also show how these estimates differ from observations. For this particular grid box, the 11 RCMs tend to produce more rainfall than observed between October and July, but less in the warmer months between July and October, and estimates of PE tend to be higher than those from MORECS. Under future projected climate change conditions the tendency for less late summer rainfall is more pronounced and there is an overall shift in the occurrence of rainfall from summer (April to September) to winter (October to March). It is assumed that any bias in the PE and rainfall estimates used to drive the G2G model will be present in both Current and Future time-slices, and thus will not be important when looking at relative changes in peak flows.

The RCM projections lie within the range of GCM projections presented in the IPCC Fourth Assessment Report (Christensen et al., 2007) which indicate that in much of Europe precipitation is likely to increase in winter but the signal in summer, especially in central and western regions is less clear (see also Rowell, 2006; Rowell and Jones, 2006; Kendon et al., 2010). Similarly, the UKCP09 report (Murphy et al., 2009) central estimates (50% probability

Fig. 5

1 level) indicate an increase in winter rainfall of 20 to 30% and a decrease in summer rainfall of  
2 20 to 30% but with an increase in summer rainfall indicated at the 10% level.

### 3 4 3.2.2 *Flood frequency*

5 In order to be able to estimate flood frequency for each river point modelled by the G2G,  
6 annual maximum (AM) flows are stored for each point by UK water-year (1 October to 30  
7 September). The AM are then ordered and their Gringorten plotting positions determined  
8 (Gringorten, 1963). A generalised logistic distribution - recommended for UK catchments by  
9 Robson and Reed (1999) - is then fitted to the AM at each point using L-moments. The fitted  
10 flood peaks can then be plotted against their return period, which is the average interval  
11 between peaks exceeding a given magnitude, to give a flood frequency curve. This method  
12 assumes stationarity over the data period, and the fitted curve should not be used for  
13 extrapolation much beyond the length of the data period.

14  
15 Flood frequency curves arising from use of RCM data as input to the G2G are presented in  
16 Fig. 6 for the four example catchments for which hydrographs were shown in Fig. 4. These  
17 curves are derived from simulations using the Current time-slice of each RCM ensemble  
18 member as input to the G2G. Also shown for each catchment is the median observed flood  
19 frequency (and its 95% bounds), derived by resampling any 30 observed (non-missing) AM  
20 daily mean flows available for the catchment between 1961 and 2005. For the Thames to  
21 Kingston the observed flood frequency curve shown is for naturalised flows, which is similar  
22 to the curve for observed flows but slightly higher, particularly at lower return periods. The  
23 comparison of observed flood frequency with RCM-derived flood frequencies (which have  
24 also been estimated using daily mean flows in this case) suggests that the flood frequency is  
25 modelled well for some catchments using (some versions of) the RCM outputs for input to  
26 G2G; but there is a tendency to over-estimate flood frequencies even for catchments for  
27 which the G2G generally performs reasonably well (such as the Ock and the Lambourne).  
28 The Darent (Fig. 4c) provides an example of a catchment for which anthropogenic influences  
29 reduce flows so significantly that the G2G overestimates, a tendency which is exacerbated  
30 through the use of RCM rainfall. It should be noted that, as for the comparison of RCM and  
31 observed rainfall and PE, the comparison of flows simulated using RCM-derived inputs with  
32 observed flows needs to be interpreted with care: the Current run of each ensemble member is  
33 not meant to reproduce exactly what happened in that period, but is simply one possible  
34 representation of what *could* have happened in that period, given the existence of stochasticity  
35 and natural variability.

Fig. 6

## 4 Results

### 4.1 Climate change impacts on flood frequency

Flood frequency curves are derived from both Current and Future time-series of 15-minute G2G-modelled river flows at each 1km river pixel, and the percentage change in peak flow at different return periods is determined. There is considerable variation in the estimated percentage change in flood frequency for different locations within the Thames Basin, between ensemble members and for different return periods. Results averaged over the 11 ensemble members are presented in Fig. 7(a): this shows the mean impact of projected climate change on peak flows at two return periods. Here it has been assumed that no ensemble member is more or less likely than any other, and so a non-weighted mean has been calculated (at each return period) from the percentage changes in flood frequency for each of the 11 ensemble members. The maps show significant variation for different parts of the Thames Basin, again highlighting the dependence of the impact on soil/geology, as areas overlying chalk (highlighted in Fig. 2) have much lower percentage changes than elsewhere. Percentage change in peak flows estimated for individual river pixels reflect the properties of the catchment draining to that location which will not necessarily be of one particular soil/geology type. However, small headwater catchments can be relatively spatially homogeneous, and it is from these that some inference can be made between catchment properties and projected future change. Specifically, examination of Fig. 7(a) indicates that percentage changes in peak flow at the 20-year return period range from -10 to 15% increase in chalk areas, from 15 to 40% in areas to the west underlain by Liassic/Oolite formations, and from 15 to 50% for London Clay. At the tidal limit of the Thames at Kingston (39001), which drains an area of mixed soil/geology/land-cover, the percentage changes in peak flow are 21% and 18% at the 5-and 20-year return periods respectively.

Fig. 7

The pattern of change across the Thames Basin is broadly in line with results obtained by Bell et al. (2009) using the G2G Model, therein denoted “Soil-G2G”, with inputs derived from a single RCM (HadRM3H) assuming UKCIP02 scenarios for the period 2070 to 2100. The differences in the two maps of projected change in peak flows across the Thames are mainly due to use of different RCM data (the UKCP09 perturbed-physics ensemble vs. a single UKCIP02 RCM run), and the emphasis here on 15-minute flows (instead of daily) for G2G model calibration and assessment. A water-balance analysis reported in Bell et al. (2009) concluded that while areas with deeper effective stores (e.g. chalk) produced similar volumes of evaporation and runoff to areas with shallower ones (e.g. London Clay), differential timing of release and partitioning of runoff between surface and sub-surface stores lead to a different

1 response. Specifically, under a possible future climate scenario of warmer drier summers and  
2 wetter winters (indicated for the 11 RCM ensemble members in Fig. 5), slowly-responding  
3 areas such as chalk will tend not to respond immediately to intense autumn/winter rainfall  
4 with high flows, but will instead replenish water in sub-surface storage. The length of the  
5 autumn/winter period required for deep stores to become replenished to field capacity would  
6 be extended further following projected increases in future evaporation. However, catchments  
7 with shallower soils, such as upland, urban and clay areas, are less affected by seasonal  
8 changes in rainfall and PE and would respond more immediately to high autumn/winter  
9 rainfall with high river flows, resulting in projected increases in future flow peaks in these  
10 areas.

11

12 One advantage of using PE and rainfall derived from a climate model with an embedded land-  
13 surface model is the ability to include climate-related processes that may be absent from  
14 simpler representations of land-atmosphere interactions. For example, the effect of projected  
15 future atmospheric CO<sub>2</sub> levels on plant stomatal conductance impacts on future estimates of  
16 PE. This effect may be an important consideration for climate impact and modelling studies  
17 since increased CO<sub>2</sub> is thought to lead to a reduction in evaporation from vegetated surfaces  
18 and a possible increase in flooding. However, most hydrological impact studies to date have  
19 neglected this effect. Six of the 11 ensemble members used here take this into account. The  
20 effect on changes in flood frequency has been determined by examining two subsets of the  
21 11-member ensemble. These subsets are:

22

23 (i) dependence of stomatal conductance on CO<sub>2</sub> ‘on’ (6 members);

24 (ii) dependence of stomatal conductance on CO<sub>2</sub> ‘off’ (5 members);

25

26 Fig. 7(c) and (d) presents maps of projected change in flood frequency for subsets (i) and (ii)  
27 respectively. When stomatal conductance of moisture flux is assumed to be dependent upon  
28 future CO<sub>2</sub> levels (subset (i)), then projected change in flood frequency is often twice as high  
29 as that for subset (ii), where independence is assumed. For subset (ii), future PE tends to be  
30 higher, particularly for summer months, resulting in drier antecedent conditions which reduce  
31 the likelihood of floods arising from autumn/winter frontal rainfall systems. For example, for  
32 the Thames at Kingston (39001), the percentage changes in 5-year return period peak flows  
33 are 20% and 10% for subsets (i) and (ii) respectively. It should be noted that detailed  
34 conclusions on the effect of specific parameter perturbations on flood frequency impacts is  
35 difficult, as multiple parameters are varied between ensemble members. However, an  
36 examination of the range of results from all 11 ensemble members allows such different  
37 possible future effects of CO<sub>2</sub> on PE to be taken into account.

1  
2  
3  
4  
5  
6  
7  
8  
9  
10  
11  
12  
13  
14  
15  
16  
17  
18  
19  
20  
21  
22  
23  
24  
25  
26  
27  
28  
29  
30  
31  
32  
33  
34  
35  
36  
37

In order to be able to better compare changes in flood frequency arising from all ensemble members, results have been extracted for each member, for each point down the main Thames and for eighteen of its principal tributaries. These have been plotted together in Fig. 8 for the 20-year return period. The bottom row shows the results for the main Thames, ‘flowing’ from left to right. Each other row includes two tributaries, which also ‘flow’ from left to right, with the right-most plotted point for each tributary being that at which it joins the main Thames (whose outlet is plotted at the far right, at position zero). The tributaries are ordered by the point at which they join the main Thames. As well as showing the results for all 11 ensemble members together, these graphs illustrate how the percentage change in peak flow varies as one moves down the rivers, and at the points where tributaries join the main Thames. In particular, this highlights the dependence of the impact on soil type, as rivers that start on chalk before flowing into clay regions have a sudden change in impact as they cross from chalk to clay (e.g. half way down the Pang, three-quarters of the way down the Kennet and one-third of the way down the Colne). Variation in the modelled flow response to rainfall and PE from different RCM ensemble members is greatest in the clay/Lias areas of the Thames Basin, and least in the chalk headwaters for which larger sub-surface stores provide some resilience to change. For all river tributaries one RCM ensemble member consistently yields unusually high PE values leading to a projected decrease in peak flows. Although PE values for this RCM are higher than for other ensemble members in both Current and Future periods, the increase in future PE coupled with relatively unchanged future annual rainfall totals leads to lower net precipitation input to catchments and projected future decreases in peak river flows.

Fig. 8

The relationship between projected climate change impacts on peak flows and underlying soil/geology is indicated in Fig. 9, where the ensemble mean percentage change in 20-year return period peak flows is plotted against the BFI of the contributing catchment for every pixel along the main river channels in the Thames Basin. Although Fig. 9 shows considerable scatter, there is a tendency for catchments with  $BFI < 0.4$  (quickly responding catchments with shallower stores) to experience increases in peak flow of 40-60% while catchments with higher BFI ( $> 0.7$ ) experience lower projected changes (5-50%). The high spatial variability in catchment soil/geology would account for the wide scatter. However, the results broadly support the conjecture that catchments with shallower soils (low BFI) would respond more immediately to high autumn/winter rainfall, yielding high river flows and resulting in high projected increases in future flow peaks for these areas. Conversely, areas with high BFI and deeper stores, such as chalk, will replenish deficits in sub-surface stores before responding to autumn/winter rainfall with increased runoff/flows.

Fig. 9

## 1 4.2 Comparison with an RCM-based estimate of current natural variability

2 An RCM ensemble for the Current time-slice can be used as input to the G2G to gain an  
3 RCM-based estimate of current natural variability in river flow, by pooling data from the  
4 ensemble. For this case, a perturbed parameter ensemble is used rather than an initial  
5 condition ensemble. The estimation has to be done with care as the simulated variables of  
6 interest from the ensemble members used need to represent samples from the same  
7 population. That is, for flood modelling they should not include any members with parameter  
8 perturbations that give very different behaviours of precipitation (or PE) metrics.

9  
10 An analysis carried out by the Met Office Hadley Centre (Elizabeth Kendon pers. comm.)  
11 suggested that a five-member subset of the original ensemble members could be pooled, as  
12 these have essentially the same settings for a number of key parameters, the perturbation of  
13 which leads to significant changes in certain precipitation characteristics. Originally six  
14 members were considered suitable for pooling, but the subset was subsequently reduced to  
15 five for the present application by excluding one member which had a different setting for the  
16 dependence of stomatal conductance on CO<sub>2</sub> to the other five ('off' versus 'on'; Fig. 7(c) and  
17 (d)). An RCM-based estimate of current natural variability has been obtained for each river  
18 point using the procedure described below.

19  
20 The AM data for the Current time-slice from the selected five-member subset are pooled. The  
21 pooled dataset is resampled with replacement into 200,002 sets of 30 AM (from the 5 by 30  
22 AM for each river point) and a flood frequency curve is fitted to each set. The differences (at  
23 specific return periods) between 100001 pairs of fitted flood frequency curves are calculated,  
24 and the bounds delineating the middle 50% and 95% are then calculated from the set of  
25 differences.

26  
27 These bounds are shown using bands of grey shading on the graphs in Fig. 8 for the 20-year  
28 return period. The modelled changes in flood frequency between the Current and Future time-  
29 slices can then be seen in the context of this estimate of the natural variability that might be  
30 expected without the presence of climate change. It can be seen that some rivers, or parts of  
31 rivers, show few changes outside the range of current natural climate variability (e.g. the  
32 Mole and the Wandle), whereas others show many changes outside the range of natural  
33 variability (e.g. the Thames and the Wey). This alters according to the return period being  
34 considered, as well as location, as is shown on the maps in Fig. 7(b): darker colours indicate  
35 areas where more of the modelled changes in peak flows are outside the range of the RCM-  
36 based estimate of natural variability. These tend to be the more hydrologically responsive

1 areas (e.g. clay and Lias formations) which have less sub-surface storage and saturate quickly  
2 during heavy rainfall.

3  
4 Locations which consistently show modelled changes outside the range of natural variability  
5 are candidates for so-called ‘early-bird’ sites, where further monitoring could be expected to  
6 show evidence of statistically significant changes in observed flows before many other sites  
7 (Wilby, 2006). However, just because a location shows few, if any, modelled changes outside  
8 the range of natural variability does not mean that it is safe from flooding in the future, as the  
9 11-member ensemble does not necessarily capture the full range of possible changes and  
10 because current flood defences may not accommodate the full range of natural variability in  
11 river flow. Also, it should be remembered that an RCM-based estimate of current natural  
12 variability has been used here as input to the G2G, and this estimate may not fully represent  
13 real variability. Natural variability could also alter under climate change.

## 14 **5 Conclusions**

### 15 **5.1 Summary**

16 The River Thames drains an area of over 10000 km<sup>2</sup> in the southeast part of England. Land-  
17 cover, soil and geology in the basin are particularly complex with a mixture of lithologies and  
18 variable land-cover including significant urban areas such as Oxford and London. The Grid-  
19 to-Grid (G2G) distributed hydrological model - formulated to employ terrain, soil and urban  
20 land-cover datasets - has been used to model river flows on a 1km grid across the Thames  
21 Basin. Model performance has been assessed with reference to high-resolution (15-minute)  
22 quality-controlled river levels/flows and using 15-minute gridded estimates of rainfall as  
23 input. The G2G model produces a realistic response to rainfall in catchments where (a) the  
24 response to rainfall is relatively free from artificial influences, (b) the river gauging station is  
25 considered to be reasonably accurate and (c) there are no significant problems with the flow  
26 and rainfall records. For these catchments,  $R^2$  Efficiency ranges from 0.59 to 0.84 (median  
27 0.77) for the calibration period and from 0.40 to 0.77 (median 0.75) for the assessment period.  
28 As the G2G primarily simulates “natural” flows, model performance can be variable for  
29 catchments with greater levels of anthropogenic disturbance.

30  
31 Following calibration and assessment on historical periods, the G2G model has been used  
32 with inputs of rainfall and PE, - estimated from the UKCP09 perturbed-parameter RCM  
33 ensemble - to simulate flood frequency across the Thames Basin. This has been done for two  
34 30-year time-slices: Current (October 1960 to September 1990) and Future (October 2069 to  
35 September 2099, under the A1B emissions scenario). Comparison of observed flood

1 frequency with RCM-derived flood frequencies for the Current period suggests that flood  
2 frequency is modelled well by most RCM ensemble members in some catchments, but over-  
3 estimates in others. However, other factors need to be borne in mind when making such a  
4 comparison, including: G2G model error, river gauging station error, the consequences of  
5 artificial influences like abstraction (not included in the G2G) on river flow records, and that  
6 the RCM Current simulations do not aim to be reproductions of the 1961-1990 period but  
7 only possible scenarios.

8  
9 The changes in flood frequency between Current and Future time-slices were then analysed  
10 on a 1km river grid across the Thames Basin. Considerable variation is evident, by ensemble  
11 member, by return period and by location, with areas underlain by chalk generally showing  
12 lower percentage changes than other regions. Almost all changes are increases, generally  
13 averaging between 5-10% in chalk areas and 30-50% elsewhere, for peak flows with up to a  
14 20-year return period. However, for one particular RCM ensemble member many changes are  
15 negative (indicating decreases in peak flow), probably due to large increases in PE. For other  
16 ensemble members changes are much higher than average, with increases of over 80% in  
17 some areas.

18  
19 It is important to recognise that projected changes in both rainfall and PE influence future  
20 changes in river flows, and that a range of methods with varying degrees of complexity are  
21 available for estimating projected future PE. In the RCM ensemble used here to estimate PE  
22 input to the hydrological model, one of the climate model parameter-perturbations of  
23 particular relevance is the dependence of stomatal conductance on atmospheric CO<sub>2</sub> levels.  
24 This effect may be an important consideration for studies of climate impact on water  
25 management as increased CO<sub>2</sub> is thought to lead to a reduction in evaporation from vegetated  
26 surfaces and a possible increase in river flow. However, most hydrological impact studies to  
27 date have neglected this effect. Six of the 11 ensemble members used here take this into  
28 account. The effect on changes in flood frequency has been determined by examining two  
29 subsets of the 11-member ensemble. If the effect of increased CO<sub>2</sub> on stomata is not taken  
30 into account, future levels of PE from vegetation are much higher and projected future change  
31 in flood frequency is lower than for the CO<sub>2</sub>-dependent subset. These differences demonstrate  
32 that it is important to consider the effect of future CO<sub>2</sub> emissions on plant physiology in  
33 addition to the effect of emissions on physical atmospheric variables such as temperature and  
34 humidity. However, it is important to note that making precise conclusions concerning the  
35 effect of specific RCM parameter-perturbations is difficult, as multiple parameters are varied  
36 between ensemble members.

37

1 Comparison of the modelled changes in flood frequency with an RCM-based estimate of  
2 current natural variability reveals that, whilst some rivers (or parts of rivers) show few  
3 changes outside of the range of current natural variability, others show many changes outside  
4 of this range. The latter locations could be considered as sites where further monitoring may  
5 provide early warning of statistically significant changes in observed flows, due to climate  
6 change. It should be remembered that an RCM-based estimate of current natural variability  
7 has been used here, which may not fully represent real natural variability. Natural variability  
8 could also alter under climate change.

## 10 **5.2 Discussion**

11 Towards the downstream end of the fluvial Thames (for example near Kingston in the vicinity  
12 of Teddington Weir), the average estimated change in modelled flood peaks for a 20-year  
13 return period is 36% with a range of -11% to +68%. These estimated changes are broadly in  
14 line with the latest guidance for England (Environment Agency, 2011), which indicates that  
15 sensitivity analyses of river flood alleviation schemes in the Thames Basin should take  
16 account of potential increases in river flood flows of 25% (median) by the 2080s, with a range  
17 of -5% to 70%. This recent guidance updates earlier FCDPAG guidance (Defra, 2006) which  
18 indicated potential increases in UK peak flows of 20% for the period 2025-2115, and was a  
19 precautionary response to the research findings of projects FD0424-C (Reynard et al., 1999)  
20 and W5-032 (Reynard et al., 2004). The Thames modelling work presented here provides  
21 further evidence of changes in peak flows that exceed 20% by the 2080s, and additionally  
22 includes the effect of increases in atmospheric CO<sub>2</sub> levels on stomatal conductance, which can  
23 result in smaller increases in PE and lead to larger increases in peak river flows.

24  
25 The large estimated increase in future peak flows should ideally be considered in a wider  
26 historical context than a modelling study over two 30-year time-slices might provide. Over  
27 the past thirty to forty years there has been some evidence of a positive trend in high river  
28 flow indicators (Hannaford and Marsh, 2008), generally thought to be linked to changes in  
29 winter precipitation arising from changes in atmospheric circulation patterns. However no  
30 such recent trend is evident for the lower Thames, and trend analyses of flow records  
31 throughout the 20<sup>th</sup> century (Black, 1996; Robson, 2002; Hannaford and Marsh, 2008) have so  
32 far detected no apparent *long-term* trend in UK flood magnitude. The modelling of current  
33 and future river flows undertaken here has relied on observations and climate model output  
34 from 1960 onwards (a period over which increases in high river flows have been detected in  
35 some areas). It is important to note that the 1961-1990 period is considered to be notably  
36 ‘flood poor’ (Hannaford and Marsh, 2008); historically flood frequencies have varied

1 substantially, a phenomenon normally assumed to be a natural consequence of the UK's  
2 inherent climatic variability. River management in recent times has led to greater channel  
3 storage and conveyance which has resulted in fewer floods in the lower Thames. The  
4 relatively low frequency of major flood events on the Thames during the 1961-1990 period  
5 indicates that the changes in return periods predicted for the 2080s should be treated with  
6 some caution, although this would be more likely to affect estimates of percentage changes  
7 from a baseline of observed flows (rather than a modelled baseline using RCM data, as  
8 applied here). Until the 1960s, snowmelt and frozen ground were major contributing factors  
9 in a significant proportion of major floods on the Thames (Griffiths, 1983) but, more recently,  
10 rising winter temperatures have resulted in a decline in snowmelt-induced flood risk in the  
11 Thames Basin (Marsh and Harvey, 2012), with significant snowfall occurring on relatively  
12 few occasions during 1961-1990. Compelling evidence for continuing temperature increases  
13 strongly suggests that snowmelt-induced flood events will continue to decline in both  
14 frequency and magnitude. The hydrological modelling undertaken here excludes the influence  
15 of snowmelt on high river flows as its impact on flood frequencies derived for the 1961-1990  
16 period in the Thames Basin is expected to be minor.

17  
18 Further development of the G2G hydrological model is ongoing, for instance through the  
19 inclusion of a snowmelt component to improve model performance, particularly for  
20 catchments located in Wales and Northern Britain. Improvements to the nature and  
21 availability of spatial datasets for soil, geology and land-cover properties will be expected to  
22 strengthen the G2G's underpinning by physical properties, and reduce reliance upon  
23 calibration of model parameters. The G2G model presented here simulates naturalised river  
24 flows and there is currently no allowance made for flood defences, or for the effect of out-of-  
25 bank flows on flood attenuation, which would in-practice lead to a reduction in high flood  
26 peaks during flood events. The introduction of a discharge-dependent wave speed and  
27 spatially variable estimates of bankfull capacity would therefore be beneficial. Such model  
28 enhancements are likely to lead to improved confidence in estimates of river flows and, in  
29 turn, improved assessment of climate change impacts on flood frequency. The inclusion of  
30 changing land-use patterns, particularly increased urbanisation, and changing patterns of  
31 abstraction could also be considered.

32  
33 Uncertainty in model estimates of the hydrological impact of climate change can arise from a  
34 range of sources including emissions scenario, model structure (for both the climate and  
35 hydrological models) and parameterisation (again for both the climate and hydrological  
36 models). For catchments considered to be particularly susceptible to increases in future flood  
37 risk, additional analysis using a catchment model (such as the PDM) adjusted for local

1 conditions is recommended. However, several studies have suggested that the greatest  
2 uncertainty comes from sources related to the modelling of the future climate, particularly the  
3 choice of GCM, rather than from emissions or hydrological modelling (Kay et al., 2008;  
4 Prudhomme and Davies, 2008; Wilby and Harris, 2006). The RCM perturbed-parameter  
5 ensemble applied in this study represents the first attempt at deriving fine-scale information  
6 consistent with a range of large-scale regional changes which result from this global  
7 modelling uncertainty. It demonstrates how these large-scale uncertainties translate into  
8 uncertainty in future flood risk. More work is required to determine how representative these  
9 assessments are of the implications of the full range of climate modelling uncertainty.

## 10 **Acknowledgements**

11 This work was undertaken for the Environment Agency under subcontract to Met Office  
12 Hadley Centre. The authors would like to thank colleagues at CEH for their help in the  
13 preparation of this paper, particularly Terry Marsh and Jamie Hannaford.  
14 Richard Jones also gratefully acknowledges funding from the Joint Department of Energy and  
15 Climate Change (DECC) and Department for Environment Food and Rural Affairs (Defra)  
16 Met Office Hadley Centre Climate Programme–DECC/Defra (GA01101).

17

## 1 **References**

2 Abbott, M.B., Bathurst, J.C., Cunge, J.A., O'Connell, P.E., Rasmussen, J., 1986. An  
3 introduction to the European Hydrological System – Système Hydrologique Européen, SHE.  
4 Structure of a physically-based distributed modelling system. *Journal of Hydrology* 87, 61-77.

5  
6 Arnell, N.W., 2003. Relative effects of multi-decadal climatic variability and changes in the  
7 mean and variability of climate due to global warming: future streamflows in Britain. *Journal*  
8 *of Hydrology* 270, 195-213.

9  
10 Bell, V.A, Gedney, N., Kay, A.L., Smith, R., Jones, R.G., Moore, R.J., 2011. Estimating  
11 potential evaporation from vegetated surfaces for water management impact assessments  
12 using climate model output. *Journal of Hydrometeorology*, in press.

13  
14 Bell, V.A., Kay, A.L., Jones, R.G., Moore, R.J., Reynard, N.S., 2009. Use of soil data in a  
15 grid-based hydrological model to estimate spatial variation in changing flood risk across the  
16 UK. *Journal of Hydrology* 377 (3-4), 335-350.

17  
18 Bell, V.A., Kay, A.L., Jones, R.G., Moore, R.J., 2007a. Development of a high resolution  
19 grid-based river flow model for use with regional climate model output. *Hydrology and Earth*  
20 *System Sciences* 11(1), 532-549.

21  
22 Bell, V.A., Kay, A.L., Jones, R.G., Moore, R.J. 2007b. Use of a grid-based hydrological  
23 model and regional climate model outputs to assess changing flood risk. *International Journal*  
24 *of Climatology* 27, 1657-1671.

25  
26 Bell, V.A., Moore, R.J., 2004. A flow routing and flood inundation facility for  
27 Nimrod/CMetS. Report to the Met Office, Centre for Ecology & Hydrology, Wallingford,  
28 UK, pp.56.

29  
30 Bell, V.A., Moore, R. J., Cole, S. J., Davies, H. N., 2008. Area-wide river flow modelling for  
31 the Thames Estuary 2100 project: Model formulation and assessment. Progress report to the  
32 Met Office (Hadley Centre), Centre for Ecology & Hydrology, Wallingford, UK, pp. 62.

33  
34 Black, A.R., 1996. Major flooding and increased flood frequency in Scotland since 1988.  
35 *Physics and Chemistry of the Earth* 20, 463-468.

36

1 Boorman, D.B., Hollis, J.M., Lilly, A., 1995. Hydrology of soil types: a hydrologically  
2 based classification of the soils of the United Kingdom. IH Report No. 126, Institute of  
3 Hydrology, Wallingford, UK, pp. 137.  
4

5 Buonomo, E., Jones, R.G., Huntingford, C., Hannaford, J., 2007. On the robustness of  
6 changes in extreme precipitation over Europe from two high resolution climate change  
7 simulations. Quarterly Journal of the Royal Meteorological Society 133 (622), 65–81.  
8

9 Cameron, D., 2006. An application of the UKCIP02 scenarios to flood estimation by  
10 continuous simulation for a gauged catchment in the northeast of Scotland, UK (with  
11 uncertainty). Journal of Hydrology 328, 212-226.  
12

13 Christensen, J.H.et al., 2007. Regional Climate Projections. In: Solomon, S. et al., (Eds.),  
14 Climate Change 2007: The Physical Science Basis. Contribution of Working Group I to the  
15 Fourth Assessment Report of the Intergovernmental Panel on Climate Change,, Cambridge  
16 University Press, Cambridge, United Kingdom and New York, NY, USA.  
17

18 Ciarapica, L., Todini, E, 2002. TOPKAPI: a model for the representation of the rainfall -  
19 runoff process at different scales. Hydrological Processes 16, 207–229.  
20

21 Cole, S.J., Moore R.J., 2008. Hydrological modelling using raingauge- and radar-based  
22 estimates of areal rainfall. Journal of Hydrology 358, 159–181.  
23

24 Cole, S.J., Moore, R.J., 2009. Distributed hydrological modelling using weather radar in  
25 gauged and ungauged basins. Advances in Water Resources 32, 1107-1120.  
26

27 Davies, H., Bell, V. 2008. Assessment of methods for extracting low resolution river  
28 networks from high resolution digital data. Hydrological Sciences Journal 54(1), 17-28.  
29

30 Defra, 2006. FCDPAG3 Economic Appraisal: Supplementary Note to Operating Authorities –  
31 Climate Change Impacts, October 2006, Department for Environment, Food and Rural  
32 Affairs, London, UK.  
33

34 De Roo, A. P. J., Wesseling, C.G., Van Deursen, W.P.A., 2000. Physically based river basin  
35 modelling within a GIS: the LISFLOOD model. Hydrological Processes 14, 1981–1992.  
36

1 De Roo, A.P.J. et al., 2003. Development of a European flood forecasting system.  
2 International Journal of River Basin Management 1(1), 49–59.  
3  
4 Dooge, J.C.I., 1973. Linear theory of hydrologic systems. Technical Bulletin 1468,  
5 Agricultural Research Service, United States Department of Agriculture, Washington, USA,  
6 pp. 327.  
7  
8 Environment Agency, 2011. Adapting to Climate Change: Advice for Flood and Coastal  
9 Erosion Risk Management Authorities. Environment Agency, September 2011, 29pp.  
10  
11 Fowler, H.J., Kilsby, C.G., 2007. Using regional climate model data to simulate historical and  
12 future river flows in northwest England. Climatic Change 80, 337-367.  
13  
14 Fuller, R.M., Smith, G.M., Sanderson, J.M., Hill, R.A., Thomson, A.G., 2002. The UK Land  
15 Cover Map 2000: Construction of a parcel-based vector map from satellite images.  
16 Cartographic Journal 39(1), 15-25.  
17  
18 Gedney, N., Cox, P.M., Betts, R.A., Boucher, O., Huntingford, C., Stott, P.A., 2006.  
19 Detection of a direct carbon dioxide effect in continental river runoff records. Nature 439,  
20 835-838.  
21  
22 Gordon, C., Cooper, C., Senior, C.A., Banks, H., Gregory, J.M., Johns, T.C., Mitchell, J.F.B.,  
23 Wood, R.A., 2000. The simulation of SST, sea ice extents and ocean heat transports in a  
24 version of the Hadley Centre coupled model without flux adjustments. Climate Dynamics 16,  
25 147-168.  
26  
27 Griffiths P.P., 1983. A chronology of Thames floods. Water Resources Report, Thames Water  
28 (Engineering Directorate), Reading, UK, pp. 54.  
29  
30 Gringorten, L.J., 1963. A plotting rule for extreme probability paper. Journal of Geophysical  
31 Research 68(3), 813–814.  
32  
33 Gustard, A., Bullock, A., Dixon, J.M., 1992. Low flow estimation in the United Kingdom.  
34 Report No. 108. Institute of Hydrology, Wallingford, UK, pp. 88.  
35  
36 Hannaford, J., Marsh, T., 2008. High-flow and flood trends in a network of undisturbed  
37 catchments in the UK. International Journal of Climatology 28, 1325-1338.

1  
2  
3  
4  
5  
6  
7  
8  
9  
10  
11  
12  
13  
14  
15  
16  
17  
18  
19  
20  
21  
22  
23  
24  
25  
26  
27  
28  
29  
30  
31  
32  
33  
34  
35  
36  
37

Henriksen, H.J., Troldborg, L., Nyegaard, P., Sonnenborg, T.O., Refsgaard, J.C., Madsen, B., 2003. Methodology for construction, calibration and validation of a national hydrological model for Denmark. *Journal of Hydrology* 280(1-4), 52-71.

Hough, M., Palmer, S., Weir, A., Lee, M., Barrie, I., 1997. The Meteorological Office Rainfall and Evaporation Calculation System: MORECS version 2.0 (1995). An update to Hydrological Memorandum 45, The Met. Office, Bracknell, UK.

Hulme, M., Jenkins, G.J., Lu, X., Turnpenny, J.R., Mitchell, T.D., Jones, R.G., Lowe, J., Murphy, J.M., Hassell, D., Boorman, P., McDonald, R., Hill, S. 2002. Climate Change Scenarios for the United Kingdom: The UKCIP02 Scientific Report. Tyndall Centre for Climate Change Research, School of Environmental Sciences, University of East Anglia, Norwich, UK.

IPCC, 2000. Special Report on Emissions Scenarios (SRES): A Special Report of Working Group III of the Intergovernmental Panel on Climate Change. Cambridge University Press, Cambridge, UK. 570pp.

IPCC 2007. Climate Change 2007: The Physical Science Basis. Contribution of Working Group I to the Fourth Assessment Report of the Intergovernmental Panel on Climate Change, Solomon, S. et al., (Eds.), Cambridge University Press, Cambridge, United Kingdom and New York, NY, USA, 996 pp.

Jenkins, G. J., Murphy, J. M., Sexton, D. M. H., Lowe, J. A., Jones, P., Kilsby, C. G., 2009. UK Climate Projections: Briefing report. Met Office Hadley Centre, Exeter, UK.

Jones, R.G., Noguer, M., Hassell, D.C., Hudson, D., Wilson, S.S., Jenkins, G.J., Mitchell, J.F.B., 2004. Generating high resolution climate change scenarios using PRECIS, Met Office Hadley Centre, Exeter, UK, pp. 40.

Kay, A.L., Davies, H.N., Bell, V.A., Jones, R.G., 2009. Comparison of uncertainty sources for climate change impacts: flood frequency in England. *Climatic Change* 92(1-2), 41-63.

Kay, A.L., Jones, R.G., Reynard, N.S., 2006. RCM rainfall for UK flood frequency estimation. II. Climate change results. *Journal of Hydrology* 318, 163-172.

1 Kendon E.J., Rowell, D.P., Jones, R.G., 2010: Mechanisms and reliability of future projected  
2 changes in daily precipitation. *Climate Dynamics* 35, 489–509, doi: 10.1007/s00382-009-  
3 0639-z  
4  
5 Marsh T.J., 2004. The January 2003 flood on the Thames. *Weather* 59(3), 59-62.  
6  
7 Marsh, T.J., Hannaford, J., 2008. The 2007 Summer Floods in England and Wales – a  
8 hydrological appraisal. Centre for Ecology & Hydrology, Wallingford, UK, 32pp.  
9  
10 Marsh, T., Harvey, C.L., 2012. The Thames flood series: a lack of trend in flood magnitude  
11 and a decline in maximum levels. *Hydrology Research* 43(3), 203–214.  
12  
13 Maraun, D., Osborn, T.J., Gillett, N.P., 2008. United Kingdom daily precipitation intensity:  
14 improved early data, error estimates and an update from 2000 to 2006. *International Journal*  
15 *of Climatology* 28(6), 833-842.  
16  
17 Monteith, J.L., 1965. Evaporation and environment. *Symposium Society for Experimental*  
18 *Biology* 19, 205-234.  
19  
20 Moore. R.J., 2007. The PDM rainfall-runoff model. *Hydrology and Earth System Sciences*  
21 11(1), 483-499.  
22  
23 Moore, R.J., Bell, V. A., Cole, S. J., Jones, D.A., 2007. Rainfall-runoff and other modelling  
24 for ungauged/low-benefit locations. Science Report SC030227/SR1, Research Contractor:  
25 CEH Wallingford, Environment Agency, Bristol, UK, pp. 249.  
26  
27 Moore, R.J., Cole, S.J., Bell, V.A., Jones, D.A., 2006. Issues in flood forecasting: ungauged  
28 basins, extreme floods and uncertainty. In: Tchiguirinskaia, I. Thein K.N.N., Hubert, P.  
29 (Eds.), *Frontiers in Flood Research*, 8th Kovacs Colloquium, UNESCO, Paris, June/July  
30 2006, IAHS Publ. 305, 103-122.  
31  
32 Moore, R.J., Bell, V.A., 2001. Comparison of rainfall-runoff models for flood forecasting.  
33 Part 1: Literature review of models. Environment Agency Research and Development  
34 Technical Report W241, Research Contractor: CEH Wallingford, Environment Agency,  
35 Bristol, UK, pp. 94.  
36

1 Moore, R.J., 1985. The probability-distributed principle and runoff production at point and  
2 basin scales. *Hydrological Sciences Journal* 30(2), 273-297.  
3

4 Murphy, J.M., Sexton, D.M.H., Jenkins, G.J., Booth, B.B.B., Brown, C.C., Clark, R.T.,  
5 Collins, M., Harris, G.R., Kendon, E.J., Betts, R.A., Brown, S.J., Humphrey, K.A., McCarthy,  
6 M.P., McDonald, R.E., Stephens, A., Wallace, C., Warren, R., Wilby, R., Wood, R.A., 2009.  
7 UK Climate Projections Science Report: Climate change projections. Met Office Hadley  
8 Centre, Exeter, UK.  
9

10 Nash, J.E., Sutcliffe, J.V., 1970. River flow forecasting through conceptual models, Part I: a  
11 discussion of principles. *Journal of Hydrology* 10(3), 282–290.  
12

13 Nawaz, N.R., Adedoye, A.J., 2006. Monte Carlo assessment of sampling uncertainty of  
14 climate change impacts on water resources yield in Yorkshire, England. *Climatic Change* 78,  
15 257-292.  
16

17 New, M., Lopez, A., Dessai, S., Wilby, R., 2007. Challenges in using probabilistic climate  
18 change information for impact assessments: an example from the water sector. *Philosophical*  
19 *Transactions of the Royal Society A* 365, 2117-2131.  
20

21 Oudin, L., Michel, H., Frederic, C., Perrin, C., Andreassian, V., Anctil, F., Loumagne, C.,  
22 2005. Which potential evapotranspiration input for a lumped rainfall–runoff model? Part 2 –  
23 Towards a simple and efficient potential evapotranspiration model for rainfall–runoff  
24 modelling. *Journal of Hydrology* 303, 290–306.  
25

26 Osborn T.J., Hulme M., 2002. Evidence for trends in heavy rainfall events over the United  
27 Kingdom. *Philosophical Transactions of the Royal Society A* 360, 1313-1325.  
28

29 Paz, A.R., Collischonn, W., Lopes da Silveira, A.L., 2006. Improvements in large-scale  
30 drainage networks derived from digital elevation models. *Water Resources Research* 42(8),  
31 doi:10.1029/2005WR004544.  
32

33 Pope V.D., Gallani M.L., Rowntree P.R., Stratton R.A., 2000. The impact of new physical  
34 parametrizations in the Hadley Centre climate model: HadAM3. *Climate Dynamics*, 16(2-3),  
35 123-146.  
36

1 Prudhomme, C., Davies, H.N., 2008. Assessing uncertainties in climate change impact  
2 analyses on river flow regimes in the UK. Part 2: future climate. *Climatic Change*, doi:  
3 10.1007/s10584-008-9461-6.  
4  
5 Reynard, N.S., Prudhomme, C., Crooks, S.M., 1999. Climate change impacts for fluvial flood  
6 defence. Report to Ministry of Agriculture, Fisheries and Food, FD0424-C, March 1999,  
7 Institute of Hydrology, Wallingford, UK, pp. 29.  
8  
9 Reynard, N.S., Prudhomme, C., Crooks, S.M., 2001. The flood characteristics of large UK  
10 rivers: potential effect of changing climate and land use. *Climatic Change* 48, 343-359.  
11  
12 Reynard, N.S., Crooks, S.M., Kay, A.L., 2004. Impact of climate change on flood flows in  
13 river catchments. Report to Department for Environment, Food and Rural Affairs and the  
14 Environment Agency, Technical Report W5-032/TR, March 2004, Centre for Ecology &  
15 Hydrology, Wallingford, UK, pp. 99.  
16  
17 Robson, A.J., Reed, D.W., 1999. Statistical procedures for flood frequency estimation. Vol. 3,  
18 Flood Estimation Handbook. Institute of Hydrology, Wallingford, UK, pp. 338.  
19  
20 Robson, A.J., 2002. Evidence for trends in UK flooding. *Philosophical Transactions of the*  
21 *Royal Society A* 360, 1327-1343.  
22  
23 Rowell, D.P., 2006. A demonstration of the uncertainty in projections of UK climate change  
24 resulting from regional model formulation. *Climatic Change*, 79, 243-257.  
25  
26 Rowell, D.P., Jones, R.G., 2006. Causes and uncertainty of future summer drying over  
27 Europe. *Climate Dynamics*, doi 10.1007/s00382-006-0125-9.  
28  
29 Thompson, N., Barrie, I.A., Ayles, M., 1982. The Meteorological Office Rainfall and  
30 Evaporation Calculation System: MORECS (July 1981). Hydrological Memorandum No. 45,  
31 Met Office, Bracknell, UK.  
32  
33 Thornthwaite, C. W., 1948. An approach toward a rational classification of climate. *American*  
34 *Geographical Review* 38, 55-94.  
35  
36 Wilby, R.L. 2006. When and where might climate change be detectable in UK river flows?  
37 *Geophysical Research Letters* 33, doi:10.1029/2006GL027552.

1

2 Wilby, R.L., Harris, I., 2006. A framework for assessing uncertainties in climate change  
3 impacts: Low-flow scenarios for the River Thames, UK. *Water Resources Research* 42, doi:  
4 10.1029/2005WR004065.

5

6 Wilby, R.L., Whitehead, P.G., Wade, A.J., Butterfield, D., Davis, R.J., Watts, G., 2006.  
7 Integrated modelling of climate change impacts on water resources and quality in a lowland  
8 catchment: River Kennet, UK. *Journal of Hydrology* 330, 204-220.

9

10 Zhao, R.J., Zuang, Y.L., Fang, L.R., Liu X.R., Zhang Q.S., 1980. The Xinanjiang model. In:  
11 *Hydrological forecasting (Proceedings. Oxford Symposium, April 1980)*, IAHS Publication  
12 129, 351-356.

13

1 **List of Tables**

2

3 Table 1 River gauging stations used for model assessment, arranged in decreasing order of  
4 BFI.

5

6

## 1 List of Figures

2

3 Fig. 1. Location map over England & Wales showing the Thames Basin with main rivers and  
4 the RCM 25km grid superimposed. The highlighted RCM grid-box to the north of the basin is  
5 referred to in Section 3.2.1.

6 Fig. 2. Thames catchment boundaries and station IDs superimposed on maps of (a) geology  
7 and (b) elevation (m).

8 Fig. 3. Calibration and assessment of G2G model performance presented in terms of  $R^2$   
9 efficiency for 34 catchments in the Thames Basin, arranged in decreasing order of BFI for (a)  
10 “undisturbed” and (b) anthropogenically-influenced catchments. Those affected by poor  
11 quality flow data during the period of assessment are indicated with a “p”.

12 Fig. 4. Sample assessment hydrographs showing modelled (red) and observed (black) river  
13 flows ( $\text{m}^3\text{s}^{-1}$ ) for four catchments. Hydrographs (a) to (c) show 15-minute flows and  
14 hydrograph (d) shows daily mean flows including naturalised flow (grey).

15 Fig. 5. Monthly mean rainfall and PE for each time-slice, and the difference between the two  
16 time-slices, for each ensemble member (solid lines), for an RCM grid-box located to the north  
17 of the Thames Basin (indicated by the highlighted box in Fig. 1). The dashed black line on the  
18 1961-1990 rainfall and PE plots indicates comparable observation data.

19 Fig. 6. Ensembles of flood frequency curves (solid lines) for four catchments in the Thames  
20 Basin, derived from G2G flow simulations using driving data from the Current time-slice of  
21 the 11-member RCM ensemble. For each catchment, the median observed flood frequency  
22 and its 95% bounds (respectively thick dashed and dotted black lines) is also shown.

23 Fig. 7. Thames Basin maps showing (at the 5- and 20-year return period) (a) percentage  
24 change in peak flows as a mean over the full 11-member ensemble; (b) number of ensemble  
25 members for which the percentage change in peak flows is above the upper 95% natural  
26 variability bound; (c) percentage change in peak flows as a mean over the six ensemble  
27 members where the dependence of stomatal conductance on  $\text{CO}_2$  is ‘on’; (d) percentage  
28 change in peak flows as a mean over the five ensemble members where the dependence of  
29 stomatal conductance on  $\text{CO}_2$  is ‘off’.

30 Fig. 8. Percentage change in 20-year return period peak flows plotted against distance from  
31 the main Thames outlet (~km), for each of the 11 ensemble members. Plots show the main  
32 Thames (bottom graph) and eighteen of its principal tributaries (left and right of other  
33 graphs). Each river ‘flows’ from left to right, with the right-most plotted point for each  
34 tributary being that at which it joins the main Thames (whose outlet is plotted at the far right,  
35 at position zero). The tributaries are ordered according to where they join the main Thames  
36 (shown in the river network map). Bands of light and dark grey shading show the extent of an  
37 RCM-based estimate of current natural variability (middle 95% and 50% respectively).

38 Fig. 9. Percentage change in 20-year return peak flows (ensemble mean) plotted against the  
39 BFI for the contributing catchment, for every pixel along the main river channels in the  
40 Thames Basin (black circles).

41

42

43

Catchment	Station ID	Area (km <sup>2</sup> )	BFI	Geology	Catchment relatively undisturbed ?	Gauge accuracy ?
Cray at Crayford	40016	119.7	0.86	Chalk/clay		Y
Lambourn at Shaw	39019	234.1	0.84	Chalk	Y	Y*
Darent at Hawley	40012	191.4	0.83	Chalk/clay		Y
Wandle at Connollys Mill	39003	176.1	0.81	Chalk/clay		
Wey at Tilford	39011	396.3	0.79	Oolite/Lias		
Windrush at Newbridge	39006	362.6	0.79	London Clay/chalk		Y
Kennet at Theale	39016	1033.4	0.76	Chalk	Y	Y*
Cherwell at Banbury	39026	199.4	0.73	Lias		
Sor Brook at Bodicote	39144	87.7	0.73	Lias	Y	Y
Wey at Weybridge	39079	1008	0.73	London Clay/chalk		N <sup>1</sup>
Mimram at Panshanger Park	38003	133.9	0.72	Chalk		Y
Ravensbourne at Catford Hill	39056	120.4	0.71	Chalk/clay		Y
Evenlode at Cassington	39034	430	0.70	Great Oolite	Y	Y
Thames at Farmoor	39129	1608.6	0.69	Oolite/Lias		Y*
Thames at Sutton Courtenay	39046	3414	0.65	Lias/Oolite/chalk		Y*
Thames at Kingston	39001	9948	0.65	Chalk/clay/etc.		Y
Ock at Abingdon	39081	234	0.64	Clay/chalk		Y*
Thames at Reading	39130	4633.7	0.64	Chalk/clay/etc.		Y
Blackwater at Swallowfield	39007	354.8	0.63	Sand/gravel/clay		Y
Colne at Denham	39010	743	0.62	Chalk/clay		
Cherwell at Enslow Mill	39021	551.7	0.59	Lias		
Cherwell at Oxford	39139	906.8	0.56	Lias /Oolite		Y
Lee at Feildes Weir	38001	1036	0.55	Chalk/clay		
Mole at Esher	39104	469.6	0.52	London Clay/sand	Y	Y
Ray at Islip	39140	290.1	0.49	Clay/Sand/Gravel		Y
Enborne at Brimpton	39025	147.6	0.49	Lias /Oolite		Y
Beverley Brook at Wimbledon Common	39005	43.5	0.47	London Clay/chalk		
Mole at Kinnersley Manor	39069	142	0.45	London Clay/sand		
Roding at Redbridge	37001	303.3	0.33	London Clay		
Mar Dyke at Stifford	37034	90.7	0.31	London Clay		
Ray at Grendon	39017	18.8	0.23	Lias	Y	Y
Cobbins Brook at Sewardstone Road	38020	38.4	0.22	London Clay		
Silkstream at Colindeep Lane	39049	29	0.18	London Clay		
Pinn at Uxbridge	39098	33.3	0.17	London Clay		

1  
2  
3

Table 1.

1  
2  
3  
4  
5  
6  
7  
8  
9  
10  
11  
12  
13  
14  
15  
16  
17  
18  
19  
20  
21  
22  
23  
24  
25  
26  
27  
28  
29  
30  
31  
32  
33  
34  
35  
36  
37  
38  
39  
40  
41  
42  
43  
44  
45  
46  
47  
48  
49  
50  
51  
52  
53  
54  
55

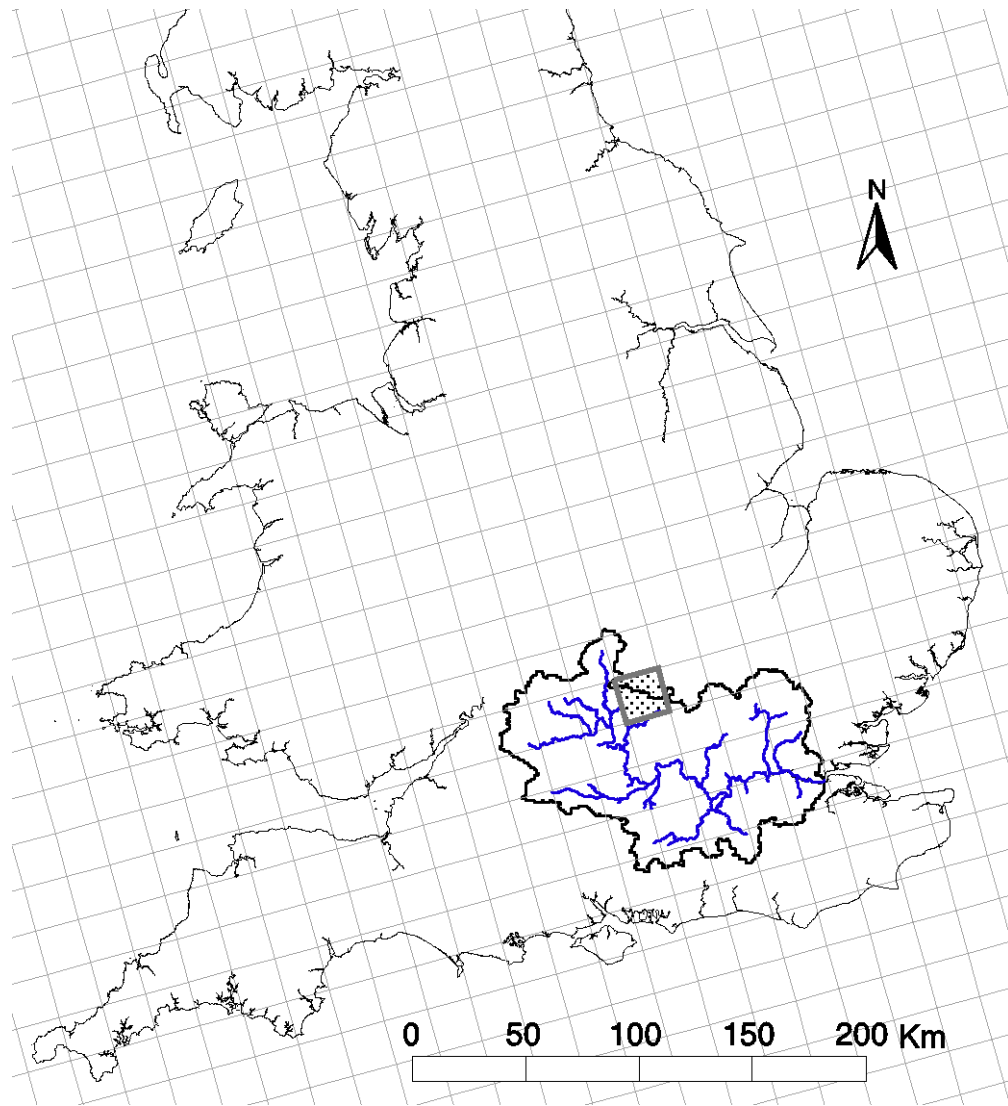


Fig. 1.

1  
2  
3  
4  
5  
6  
7  
8  
9  
10  
11  
12  
13  
14  
15  
16  
17  
18  
19  
20  
21  
22  
23  
24  
25  
26  
27  
28  
29  
30  
31  
32  
33  
34  
35  
36  
37  
38  
39  
40  
41  
42  
43  
44  
45  
46  
47  
48  
49  
50  
51  
52  
53  
54  
55

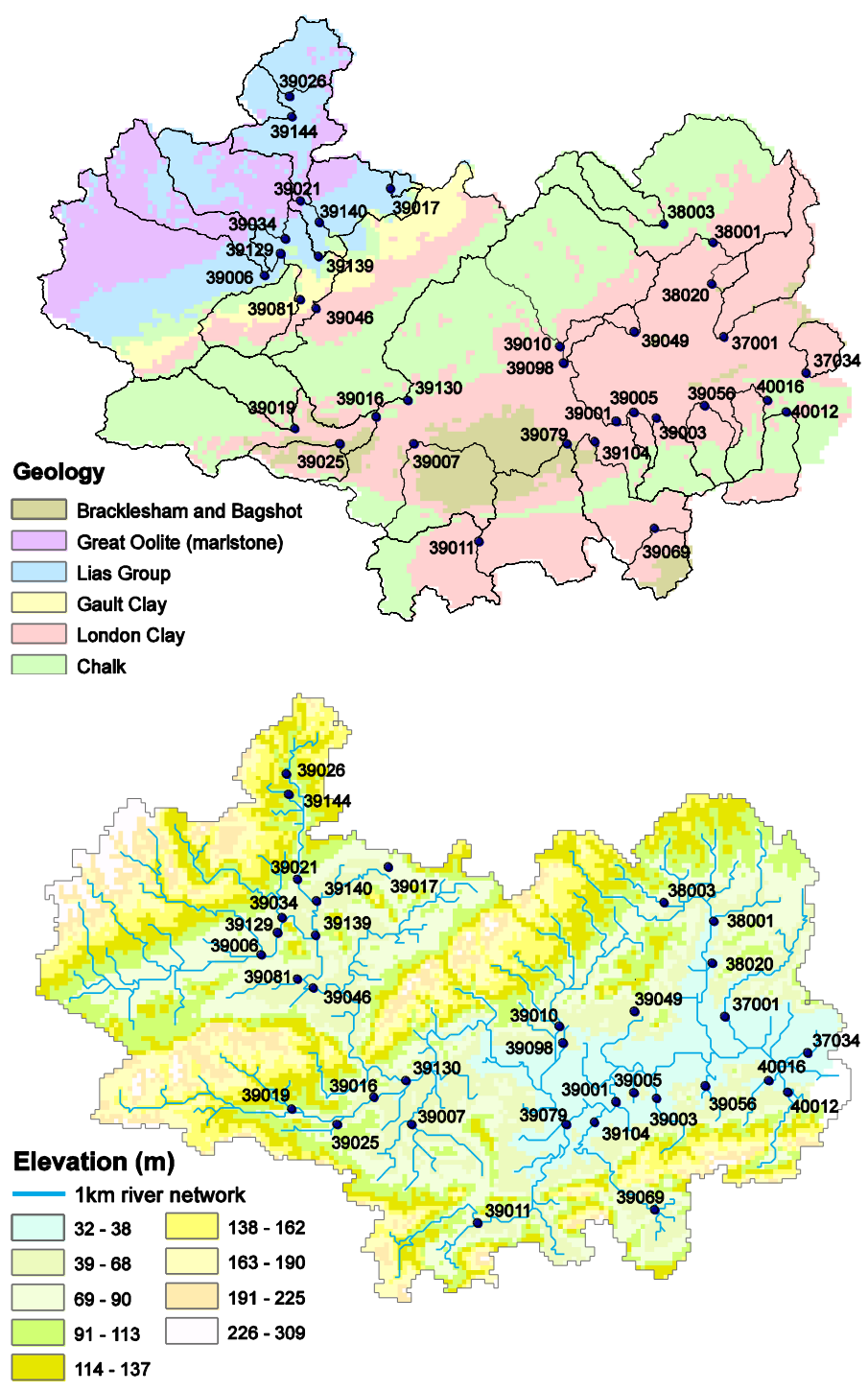
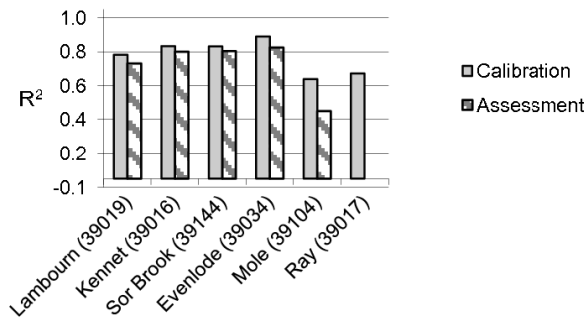


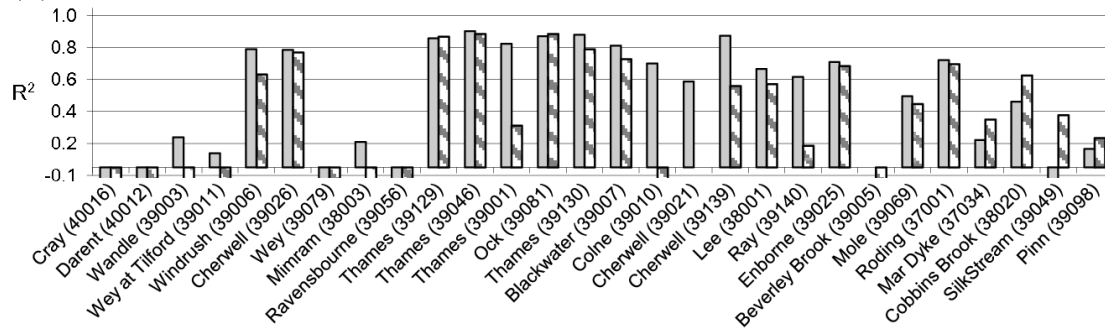
Fig. 2.

1

(a) Undisturbed basins



(b) Anthropogenically-influenced basins

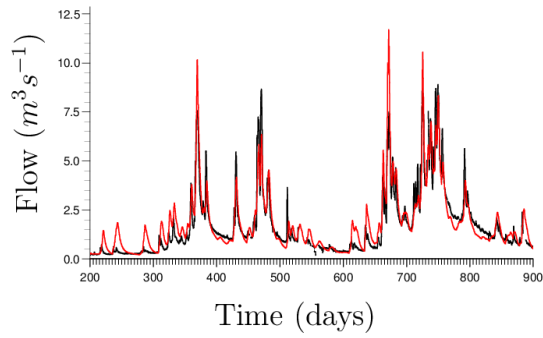


2  
3  
4  
5  
6  
7  
8  
9  
10  
11  
12  
13  
14  
15  
16  
17  
18  
19  
20  
21  
22  
23  
24  
25  
26  
27  
28  
29  
30  
31  
32  
33  
34

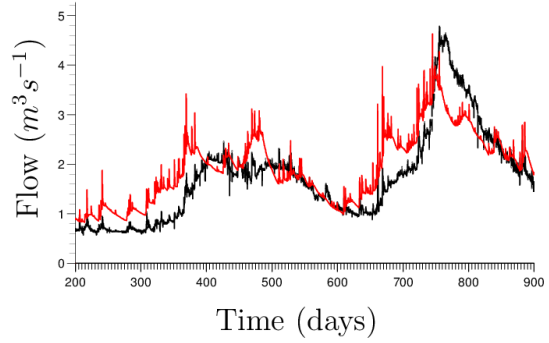
Fig. 3.

1  
2

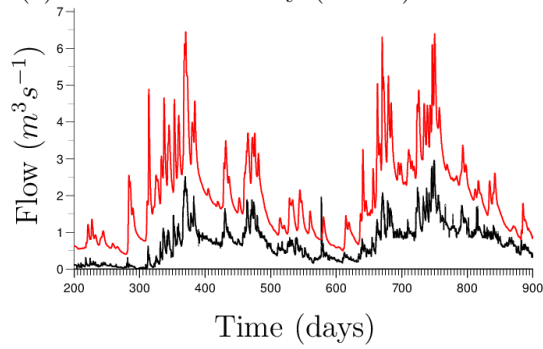
(a) Ock at Abingdon (39081)



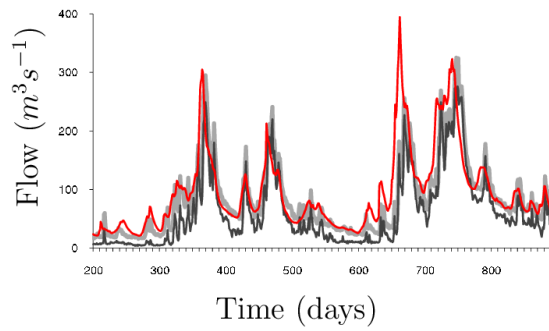
(b) Lambourn at Shaw (39019)



(c) Darent at Hawley (40012)



(d) Thames at Kingston (39001)



3  
4  
5  
6  
7  
8  
9  
10  
11  
12  
13  
14  
15  
16  
17  
18  
19  
20  
21  
22  
23  
24  
25  
26  
27  
28  
29  
30  
31  
32

Fig.4.

1  
2  
3  
4  
5  
6  
7  
8  
9  
10  
11  
12  
13  
14  
15  
16  
17  
18  
19  
20  
21  
22  
23  
24  
25  
26  
27  
28  
29  
30  
31  
32  
33  
34  
35  
36  
37  
38  
39  
40  
41  
42  
43  
44  
45  
46  
47  
48  
49  
50  
51  
52  
53  
54  
55

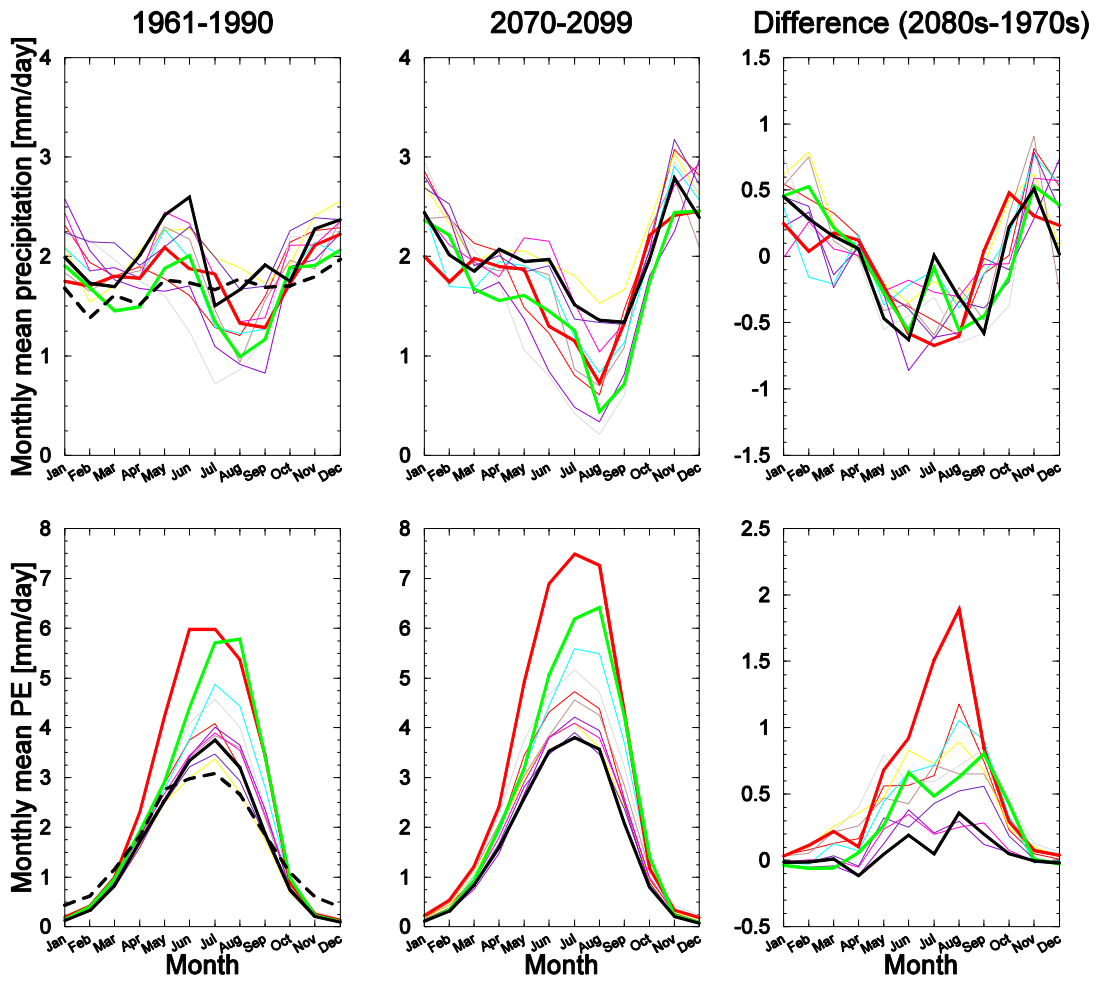
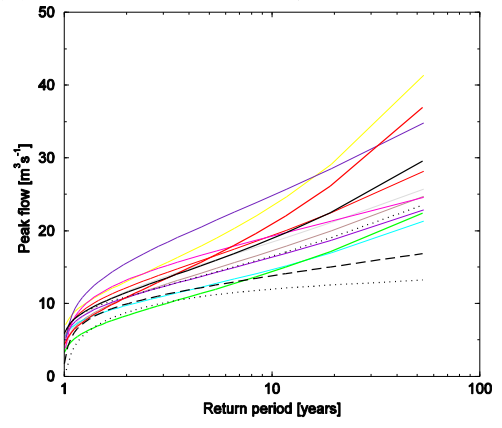


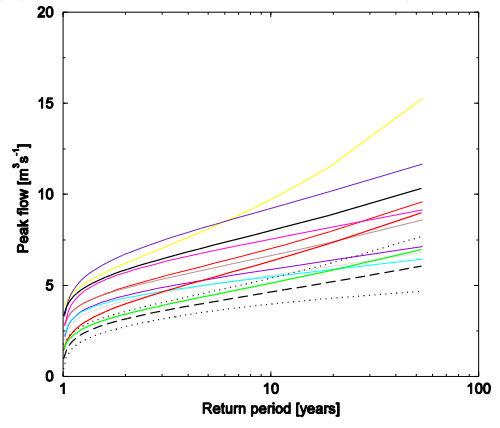
Fig. 5.

1  
2  
3  
4  
5  
6  
7  
8  
9  
10  
11  
12  
13  
14  
15  
16  
17  
18  
19  
20  
21  
22  
23  
24  
25  
26  
27  
28  
29  
30  
31  
32  
33  
34  
35  
36  
37  
38  
39  
40  
41  
42  
43  
44  
45  
46  
47  
48  
49  
50  
51  
52  
53  
54  
55

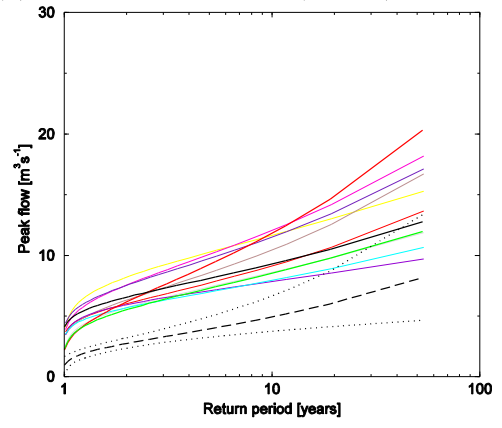
(a) Ock at Abingdon (39081)



(b) Lambourn at Shaw (39019)



(c) Darent at Hawley (40012)



(d) Thames at Kingston (39001)

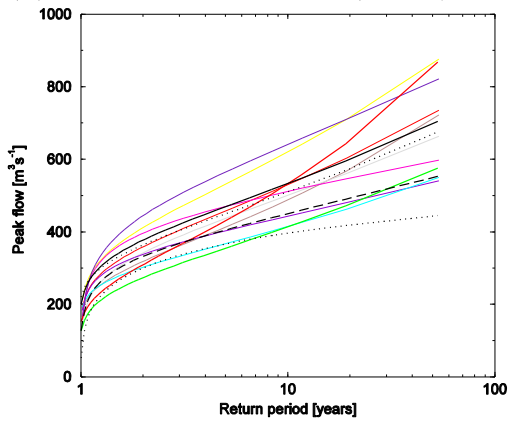


Fig. 6.

1  
2  
3  
4  
5  
6  
7  
8  
9  
10  
11  
12  
13  
14  
15  
16  
17  
18  
19  
20  
21  
22  
23  
24  
25  
26  
27  
28  
29  
30  
31  
32  
33  
34  
35  
36  
37  
38  
39  
40  
41  
42  
43  
44  
45  
46  
47  
48  
49  
50  
51  
52  
53  
54  
55

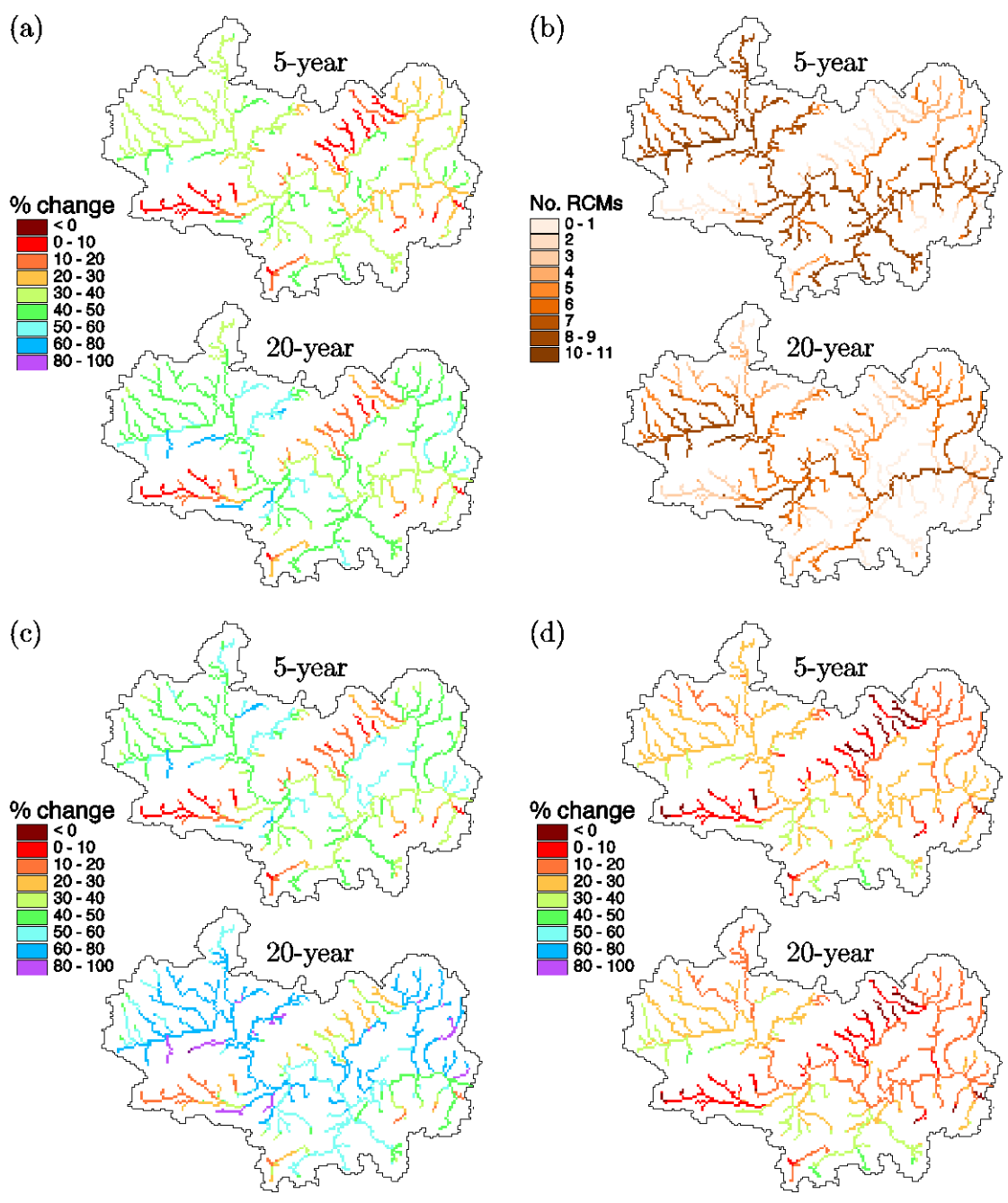
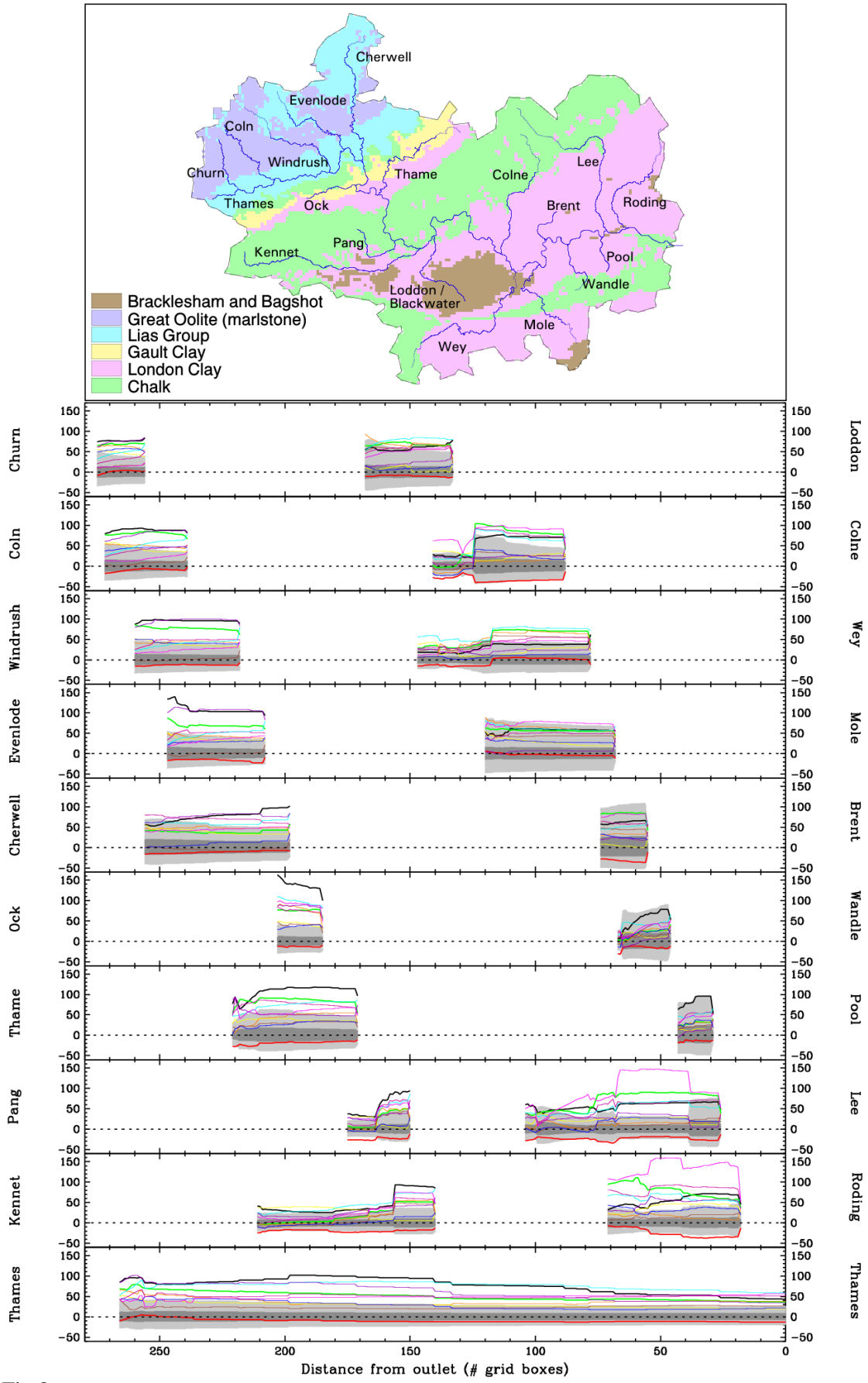
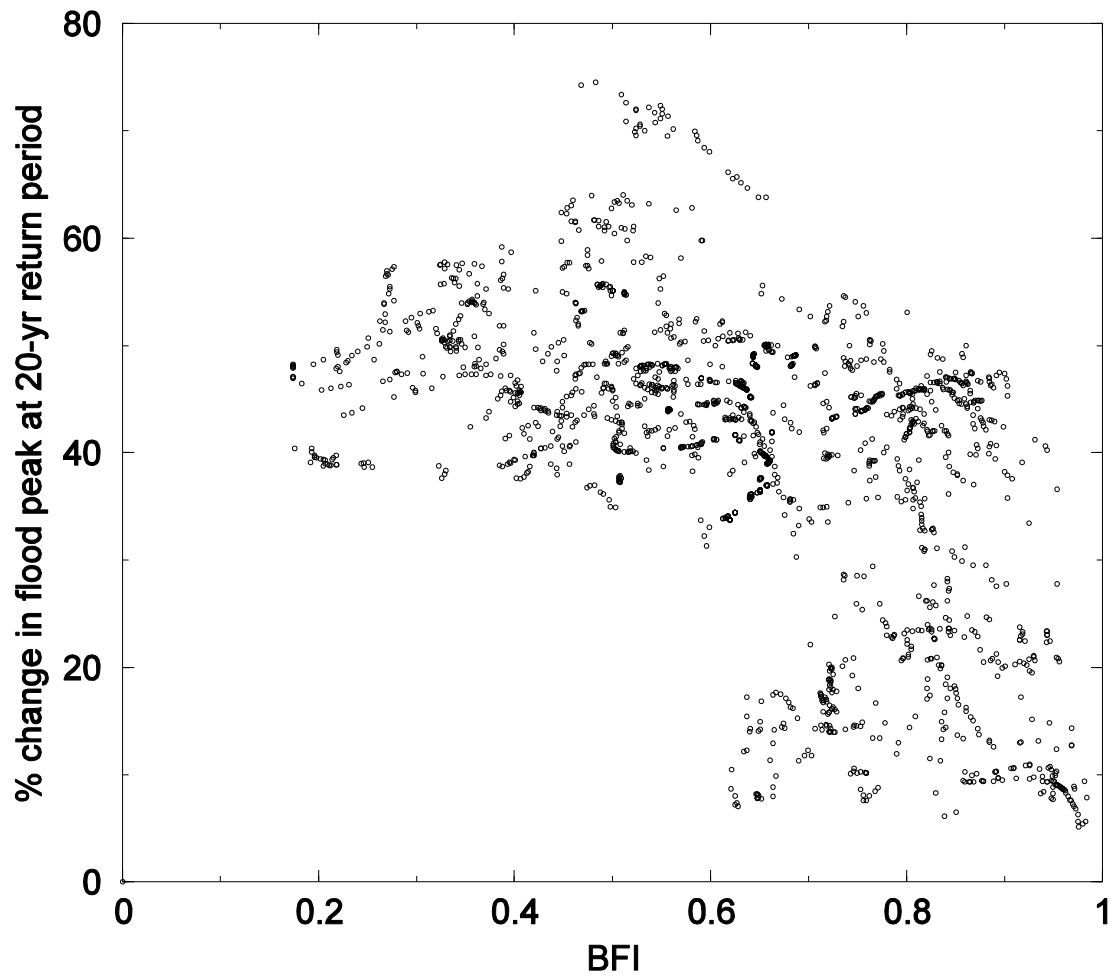


Fig. 7.



2  
3 Fig.8.

1  
2



3  
4  
5  
6  
7

Fig.9.